

See discussions, stats, and author profiles for this publication at: <https://www.researchgate.net/publication/267456343>

Design, synthesis and in vitro evaluation of novel dehydroabietic acid derivatives containing a dipeptide moiety as potential anticancer agents

ARTICLE *in* EUROPEAN JOURNAL OF MEDICINAL CHEMISTRY · JANUARY 2015

Impact Factor: 3.45 · DOI: 10.1016/j.ejmech.2014.10.060

CITATIONS

2

READS

53

8 AUTHORS, INCLUDING:



Ye Zhang

Guilin Normal College

38 PUBLICATIONS 201 CITATIONS

SEE PROFILE



Ying ming Pan

Guangxi Normal University

121 PUBLICATIONS 1,020 CITATIONS

SEE PROFILE



Contents lists available at ScienceDirect

European Journal of Medicinal Chemistry

journal homepage: <http://www.elsevier.com/locate/ejmech>

Original article

Design, synthesis and *in vitro* evaluation of novel dehydroabietic acid derivatives containing a dipeptide moiety as potential anticancer agentsXiao-Chao Huang^{a,1}, Le Jin^{a,1}, Meng Wang^a, Dong Liang^a, Zhen-Feng Chen^a, Ye Zhang^{a,b}, Ying-Ming Pan^{a,*}, Heng-Shan Wang^{a,*}^a State Key Laboratory Cultivation Base for the Chemistry and Molecular Engineering of Medicinal Resources, School of Chemistry and Pharmaceutical Science of Guangxi Normal University, Yucai Road 15, Guilin 541004, Guangxi, PR China^b Department of Chemistry and Pharmaceutical Science, Guilin Normal College, Xinyi Road 21, Guangxi 541001, PR China

ARTICLE INFO

Article history:

Received 2 March 2014

Received in revised form

17 October 2014

Accepted 20 October 2014

Available online 22 October 2014

Keywords:

Dehydroabietic acid

Dipeptide

Chiral

Antitumor

Apoptosis

ABSTRACT

A series of novel dehydroabietic acid (DHA) chiral dipeptide derivatives were designed and synthesized as potent antitumor agents. The inhibitory activities of these compounds against NCI–H460 (lung), HeLa (epithelial cervical) and MGC-803 (gastric) human cancer cell lines were estimated by MTT assay *in vitro*. The antitumor activities screening indicated that many compounds showed moderate to high levels of antitumor activities against these three cancer cell lines and most of these compounds displayed more potent inhibitory activities compared with commercial anticancer drug 5-fluorouracil (5-FU). The induction of apoptosis and effects on the cell cycle distribution with compound **8k** were investigated by acridine orange/ethidium bromide staining, Hoechst 33258 staining, JC-1 mitochondrial membrane potential staining, TUNEL assay, flow cytometry and the activities of caspase-3 and -9 assay in HeLa cells, which exhibited that the compound could induce cell apoptosis in HeLa cells. In addition, further investigation showed that apoptosis were associated with loss of mitochondrial membrane potential, enhancement of mitochondrial cytochrome c release and intracellular ROS production, elevation of Bax expression, down-regulation of Bcl-2, and the activation of caspase-9 and -3.

© 2014 Elsevier Masson SAS. All rights reserved.

1. Introduction

Cancer, being one of the leading causes of death globally, is a disease of worldwide importance. As a result, there is a consistent need of searching novel molecules with anticancer effective. Natural products played an important role in drugs discovery, especially in the area of cancer pharmacology. They are still major source of new antitumor drugs development, and many natural or natural based antitumor drugs such as taxol, vinblastine, bleomycin and doxorubicin derivatives were clinically used in recent year [1–3]. Encouraged by these research results, our interest in investigating natural products for their potential therapeutic effects has recently spurred us to examine the influences of dehydroabietic acid derivatives on antitumor properties.

DHA is a natural occurring diterpenic resin acid, which can be easily isolated from commercial disproportionated rosin [4]. Recent reports indicate that DHA and its derivatives exhibited wide range of biological activities, such as antiulcer, antimicrobial, antifungal, anti-inflammatorily, anti-pepsin, anxiolytic, antiviral, antitumor, and cytotoxic activities [5–11]. Modern studies have indicated that DHA and some derivatives have been reported to have anticancer activity in many human cancer cells such as cervical carcinoma cells, hepatocellular carcinoma cells and breast cancer cells, as well as its analogs [12,13]. Previous work has also found that the introduction of functional groups ureas in carboxylic acid group of DHA would improve antitumor activity [14]. Furthermore, in our previous work, it has found that the introduction of functional groups thiourea or/and α -aminophosphonate groups in carboxylic acid group of DHA showed improved antitumor activity [15]. As a result, our present work in this paper is to design and synthesize a new class of DHA derivatives, and to evaluate their *in vitro* anticancer activities.

Peptides play crucial roles in the human body and other organisms [16]. Previous work indicated that dipeptides and their

* Corresponding authors.

E-mail addresses: panym2013@hotmail.com (Y.-M. Pan), whengshan@163.com (H.-S. Wang).¹ Co-first author: These authors contributed equally to this work.

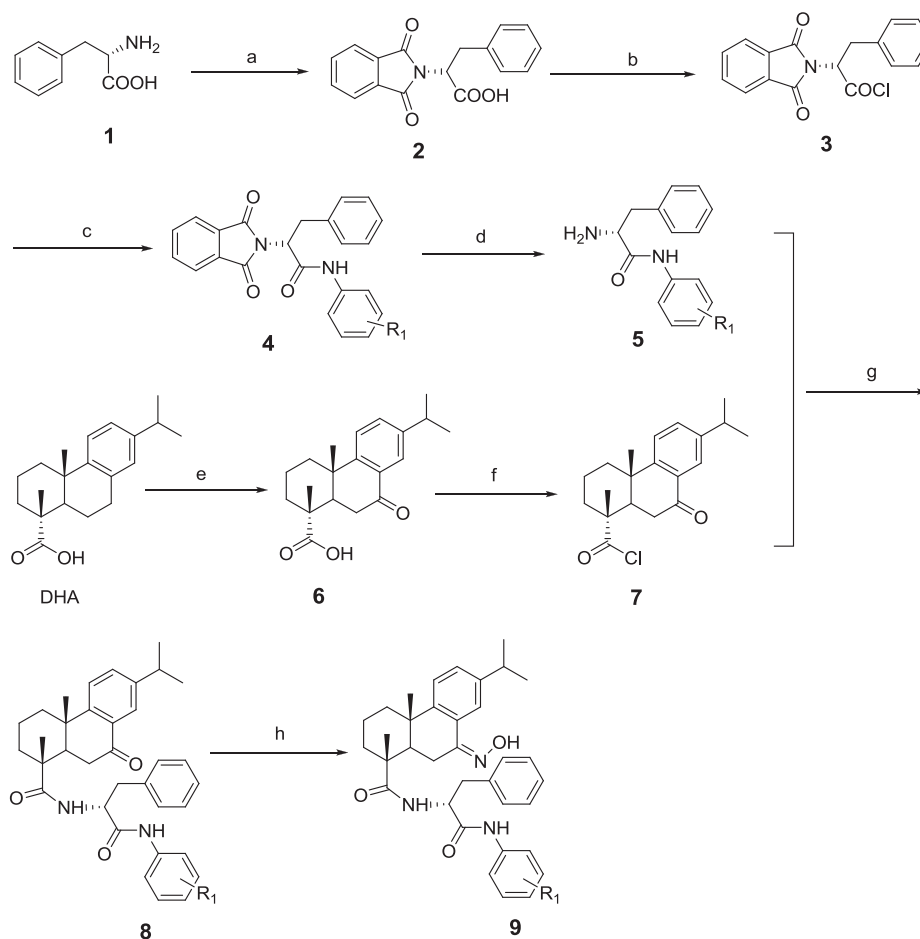
derivatives have exhibited a wide spectrum of important bioactivities such as antimicrobial, neuroprotective, antiviral and anticancer activities [17–19]. Peptides are among the most versatile bioactive molecules e.g. many peptide hormones and analogous short peptides exert their action by binding to membrane receptors [20,21]. However, most of natural peptides consists of L-form α -amino acids and due to the ubiquitous prevalence of peptidases, they exhibit limited biostability, and consequently low bioavailability [21]. To solve this problem, other stable and biologically active peptides have been thus developed. Several L- and D-amino acids have been thus introduced into the natural products skeleton, and such analogs as conjugates of paclitaxel, doxorubicin and daunorubicin with an amino acid or peptides have been demonstrated increased and more selective anticancer activity than the drugs themselves [22–26]. In addition, previous work demonstrated that many oxime derivatives exhibited good antitumor activity and the introduction of oxime group to some active core skeleton may lead to better antitumor activity [27,28]. So in this paper, as a development of the previous research work [29], we have designed and synthesized a series of new DHA dipeptide derivatives containing oxime group. Their cytotoxicities *in vitro* against three selected tumor cell lines were evaluated. Results showed that the target compounds can inhibit proliferation on these three tumor cell lines at moderate to high rates. Moreover, our results clearly demonstrated that compound **8k** can induce apoptosis in HeLa cells. Furthermore, the related molecular

mechanism involving the apoptosis effects induced by **8k** was also investigated.

2. Results and discussion

2.1. Chemistry

A new class of novel DHA chiral dipeptide derivatives were synthesized as outlined in Scheme 1. The synthetic route to the targeted molecule is simple, concise, and high yielding. Compound **2** was synthesized by the treatment of phenylalanine **1** with phthalic anhydride in the presence of acetic acid according to the literature [30]. Compound **3** was then obtained by the condensation of compound **2** and oxalyl chloride, and it was then treated with series of aromatic primary amines to offer compounds **4**. Compounds **5** were synthesized by the treatment of compounds **4** with hydrazine hydrate in the presence of ethanol at room temperature. 7-Oxo-dehydroabietic acid **6** was synthesized by the treatment of dehydroabietic acid with chromic anhydride in the presence of glacial acetic acid [31]. 7-Oxo-dehydroabietic acid was treated with oxalyl chloride to offer compound **7**. Compounds **8** were finally acquired by the condensation of compound **7** and compounds **5** in the presence of triethylamine at room temperature. Compounds **9** were finally acquired by the condensation of compounds **8** with hydroxylamine hydrochloride in the presence of ethanol at 80 °C. The structures of DHA dipeptide derivatives **8–9**



Scheme 1. Synthetic pathway to target compounds **8a–8p** and **9a–9p**. Reagents and conditions: (a) phthalic anhydride, CH_3COOH , 50 °C; (b) oxalyl chloride, CH_2Cl_2 , r.t.; (c) aromatic primary amines, Et_3N , CH_2Cl_2 , r.t.; (d) hydrazine hydrate, CH_3OH ; (e) CrO_3 , CH_3COOH , r.t.; (f) oxalyl chloride, CH_2Cl_2 , r.t.; (g) Et_3N , CH_2Cl_2 , r.t.; (h) hydroxylamine hydrochloride, $\text{CH}_3\text{CH}_2\text{OH}$, 80 °C.

Table 1
Effect of compounds **8a–8p** and **9a–9p** against cell viability of different cell lines.

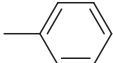
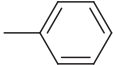
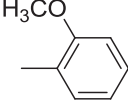
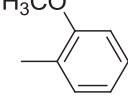
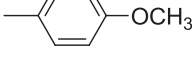
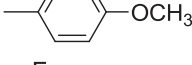
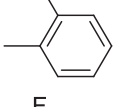
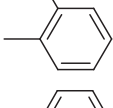

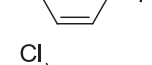
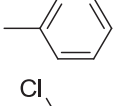
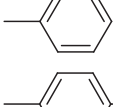
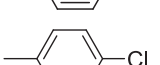
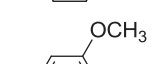
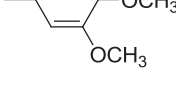
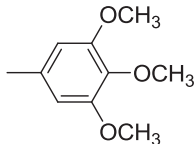
Compound	IC ₅₀ (μM)					
	L- and D-	R ₁	HeLa	NCI-H460	MGC-803	HL-7702
8a	L-		29.06 ± 2.4	28.98 ± 3.1	27.61 ± 2.6	51.59 ± 1.2
8b	D-		57.83 ± 3.2	51.94 ± 4.5	30.46 ± 4.3	53.27 ± 2.2
8c	L-		14.72 ± 1.5	33.84 ± 1.6	39.38 ± 2.4	57.46 ± 1.6
8d	D-		40.71 ± 3.2	85.40 ± 5.4	30.90 ± 2.3	55.69 ± 2.3
8e	L-		52.31 ± 3.5	>100	48.95 ± 2.7	59.61 ± 2.7
8f	D-		16.32 ± 1.3	34.34 ± 1.8	39.58 ± 3.7	55.41 ± 3.5
8g	L-		18.92 ± 1.4	57.10 ± 3.6	18.89 ± 2.2	47.57 ± 4.3
8h	D-		25.86 ± 2.5	61.43 ± 4.2	18.90 ± 1.0	53.31 ± 3.3
8i	L-		63.48 ± 5.3	61.63 ± 4.0	20.11 ± 1.2	66.45 ± 2.5
8j	D-		16.32 ± 2.1	34.32 ± 1.8	39.58 ± 3.4	52.42 ± 4.9
8k	L-		7.76 ± 0.98	24.33 ± 1.7	9.70 ± 1.4	53.78 ± 1.4
8l	D-		>100	49.97 ± 3.5	29.70 ± 2.6	46.54 ± 1.9
8m	L-		35.95 ± 3.2	49.05 ± 4.6	28.99 ± 3.1	57.82 ± 3.2
8n	D-		32.26 ± 3.4	23.41 ± 2.6	20.23 ± 1.5	76.32 ± 1.8
8o	L-		49.59 ± 2.4	54.59 ± 4.4	21.32 ± 2.0	69.46 ± 1.3

Table 1 (continued)

Compound	IC ₅₀ (μM)					
	L- and D-	R ₁	HeLa	NCI-H460	MGC-803	HL-7702
8p	D-		19.17 ± 1.4	27.92 ± 1.8	26.39 ± 2.9	57.41 ± 3.3
9a	L-		15.96 ± 1.0	41.34 ± 2.0	16.00 ± 1.3	45.89 ± 1.2
9b	D-		12.51 ± 1.5	33.09 ± 2.5	13.45 ± 1.4	48.20 ± 3.2
9c	L-		19.26 ± 1.7	30.99 ± 2.5	11.86 ± 1.2	58.76 ± 3.5
9d	D-		18.42 ± 1.5	37.09 ± 2.5	18.71 ± 1.4	57.89 ± 2.2
9e	L-		10.86 ± 0.52	32.05 ± 1.4	14.59 ± 1.6	49.56 ± 1.9
9f	D-		17.30 ± 1.7	20.38 ± 1.8	15.04 ± 0.85	56.25 ± 1.9
9g	L-		34.11 ± 3.4	44.80 ± 3.5	17.84 ± 2.5	57.53 ± 3.7
9h	D-		20.78 ± 2.8	42.47 ± 2.1	13.44 ± 1.2	54.83 ± 2.6
9i	L-		20.65 ± 0.92	23.37 ± 3.1	24.40 ± 3.7	49.67 ± 2.7
9j	D-		20.56 ± 1.8	58.61 ± 4.1	17.26 ± 1.5	53.77 ± 3.2
9k	L-		22.81 ± 1.9	36.45 ± 2.8	22.36 ± 1.8	45.89 ± 1.2
9l	D-		26.56 ± 2.7	26.86 ± 3.3	17.01 ± 1.6	48.20 ± 3.2
9m	L-		101.24 ± 2.3	102.26 ± 3.1	25.76 ± 1.9	60.82 ± 3.2
9n	D-		20.18 ± 1.8	17.61 ± 2.4	17.80 ± 2.3	57.89 ± 2.2
9o	L-		25.92 ± 1.4	36.61 ± 3.0	17.53 ± 1.9	49.56 ± 1.9

(continued on next page)

Table 1 (continued)

Compound	IC ₅₀ (μM)		HeLa	NCI–H460	MGC-803	HL-7702
	L- and D-	R ₁				
9p	D-		32.03 ± 1.9	36.12 ± 3.8	15.62 ± 2.6	56.25 ± 1.9
DHA			29.35 ± 3.4	84.53 ± 4.5	>100	ND
5-FU			36.53 ± 1.8	36.04 ± 2.2	30.45 ± 2.9	ND

ND: Not detect.

were confirmed by ¹H NMR, ¹³C NMR and high resolution mass spectrum (HR-MS).

2.2. Evaluation of antitumor activities

The *in vitro* cytotoxic potency of DHA chiral dipeptide derivatives **8**–**9** were evaluated by MTT assay against NCI–H460, HeLa and MGC-803 tumor cell lines, with 5-fluorouracil (5-FU) as the positive control. All the tested target compounds were dissolved in DMSO and subsequently diluted in culture medium before treatment of cultured cells. The control cells were treated with culture medium containing 0.1% DMSO. The values of IC₅₀, the effective concentration at which 50% of the tumor cells were inhibited, were calculated to evaluate the antitumor activities. If 50% inhibition could not be reached at the highest concentration, then >100 μM was given. The tested results were shown in Table 1.

As shown in Table 1, most of DHA dipeptide derivatives **8a**–**8p** and **9a**–**9p** displayed much higher inhibitory activity than DHA against the HeLa, NCI–H460 and MGC-803 cancer cell lines, indicating the introduction of L- and D- Phenylalanine derivatives on DHA should markedly improve the antitumor activity. In addition, by the comparison of IC₅₀ values of compounds **8** with **9**, from Table 1 it is evident that C=N–OH group in 7 position of DHA skeleton was an important contributor to their cytotoxic activities. Table 1 also revealed that, in HeLa cell line assay, most of the compounds (such as **8a**, **8c**, **8f**–**8h**, **8j**, **8p**, **9a**–**9l**, **9n** and **9o**) exhibited better inhibition than DHA (IC₅₀ = 29.35 μM), and even displayed preferable cytotoxic activities than the commercial anticancer drug 5-FU (IC₅₀ = 36.53 μM), with IC₅₀ in the range of 7.76–29.06 μM, respectively. The cytotoxic inhibition screening results demonstrated that the introduction of L- and D- phenylalanine derivatives on DHA could markedly improve the antitumor activity against HeLa cancer cell line. From the data, selected chiral compounds L-**8k**, D-**9b** and L-**9e** were exhibited the best cytotoxicity, with IC₅₀ of 7.67, 12.51 and 10.86 μM.

In NCI–H460 cancer cell line assay, most of compounds (except compounds **8d**, **8e** and **9m**) displayed better cytotoxicity than DHA (IC₅₀ = 84.53 μM), with IC₅₀ in the range of 17.61–61.63 μM, indicating that the introduction of L- and D- Phenylalanine derivatives on DHA should improve the antitumor activity against NCI–H460 cancer cell line. Moreover, some of compounds even demonstrated better cytotoxic inhibition than 5-FU, implying favorable inhibition activities of these compounds. Among these compounds, compound **9n** showed the best inhibition, with IC₅₀ of 17.61 μM.

In MGC-803 cancer cell line assay, all compounds displayed better cytotoxicity than DHA (IC₅₀ > 100 μM), with IC₅₀ in the range of 9.70–48.95 μM, indicating that the introduction of L- and D- Phenylalanine derivatives on DHA should improve the anti-proliferative activity against MGC-803 cells. Moreover, most of compounds even demonstrated better cytotoxic inhibition than 5-FU, such as compound **8k** displayed the best inhibition on MGC-803 cell line among all the compounds, with IC₅₀ of 9.70 μM. In addition, as shown in Table 1, these derivatives showed similar inhibition activity against the HeLa, NCI–H460 cancer cell lines, while the proliferation inhibition of MGC-803 cancer cells was superior to other kinds of cancer cell lines.

The inhibition activities of compounds **8** and **9** against HL-7702 normal human liver cell lines were also estimated. The data of MTT assay against HL-7702 cell lines were listed in Table 1. The results indicated that most of compounds showed a low cytotoxicity on HL-7702 cells (with IC₅₀ in the range of 45.89 ± 1.2–87.80 ± 1.5 μM) and high antitumor *in vitro* activity on the three cancer cell lines. In addition, target compound **8k** displayed the highest cytotoxicity against HeLa cancer cells with IC₅₀ values of 7.76 ± 0.98 μM and showed a low cytotoxicity against HL-7702 cells with IC₅₀ values of 53.78 ± 1.4 μM, making them good candidates as antitumor drugs. These results indicated that the targeted compounds have selective and significant effect on the cell lines.

Based on the above observation, some interesting structure-activity relationships could be concluded: (1) the introduction of

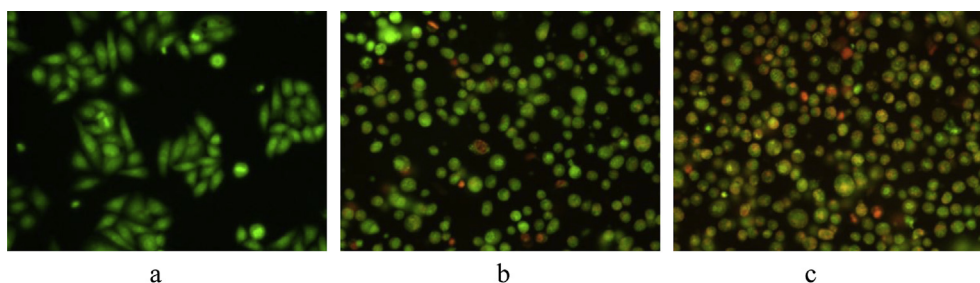


Fig. 1. AO/EB staining of compound **8k** in HeLa cells. (a) Not treated with the **8k** were used as control at for 24 h and (b, c) treatment with compound **8k** (15 μM) for 12 h and 24 h, respectively.

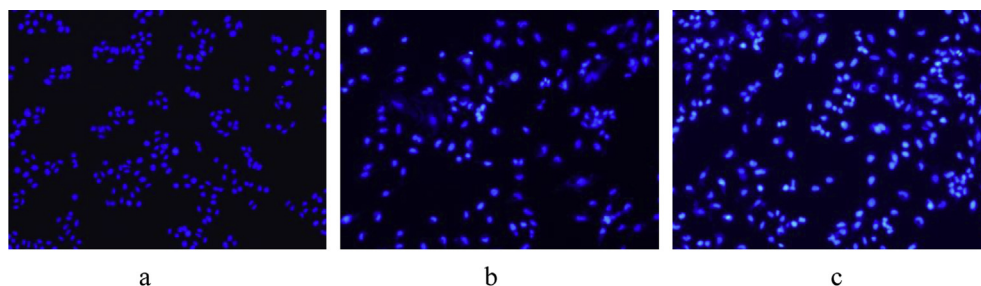


Fig. 2. Hoechst 33258 staining of compound **8k** in HeLa cells. (a) Not treated with compound **8k** were used as control at for 24 h and (b, c) treatment with compound **8k** (15 μ M) for 12 h and 24 h, respectively.

dipeptide was significant for improving their activity; (2) compared the antitumor activity of compounds **8** with **9**, it could be found that the antitumor activity of compounds **9** were better than that of **8**. It was important to note that C=N–OH group in **7** position of DHA skeleton was important for improving antitumor activities; (3) it could be found that most ortho-substitution in the phenyl group of phenylalanine favored the L-conformer whereas para-substitution in the phenyl group favored the D-conformer.

2.3. Investigation of apoptosis

Apoptosis plays a central role in cancer, since its induction in cancer cells is important to a successful therapy [32]. It is thus

considered that apoptosis assay could provide important information to the study of the mode of action. In our previous work, it has been reported that DHA derivatives induce apoptosis and growth inhibition at the G1 phase of the cell cycle in NCI–H460 cancer cell line [15]. Therefore, in our present study, compound **8k** which exhibited good cytotoxic inhibition in HeLa cancer cell line and could be used as a good representative of compounds **8a–8p** and **9a–9p** was selected to analyze the mechanism of growth inhibition of HeLa cells by the following methods.

2.3.1. Fluorescence staining

Changes in the morphological character of HeLa cells were studied using acridine orange (AO)/ethidium bromide (EB),

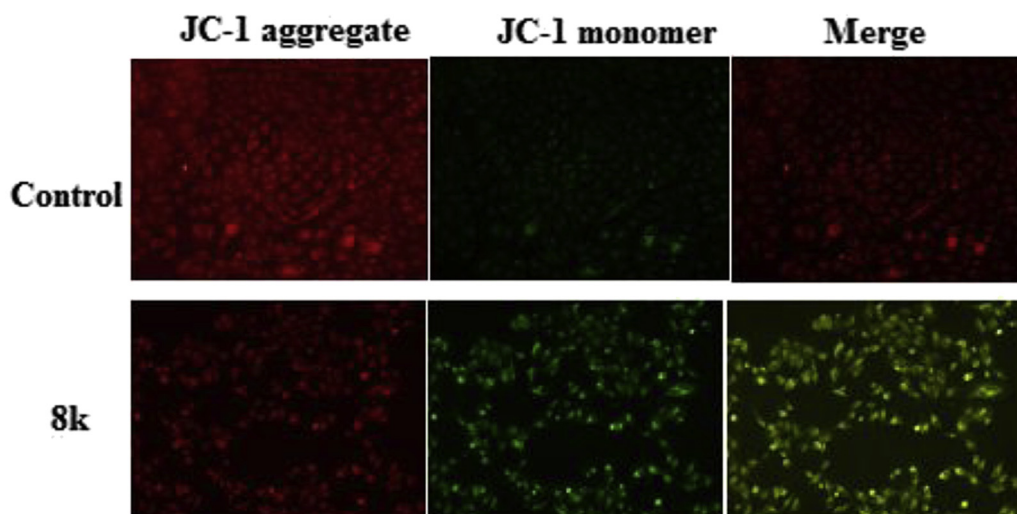


Fig. 3. JC-1 mitochondrial membrane potential staining of compound **8k** in HeLa cells. Not treated with the **8k** were used as control at for 24 h and treatment with compound **8k** (15 μ M) for 24 h, respectively.

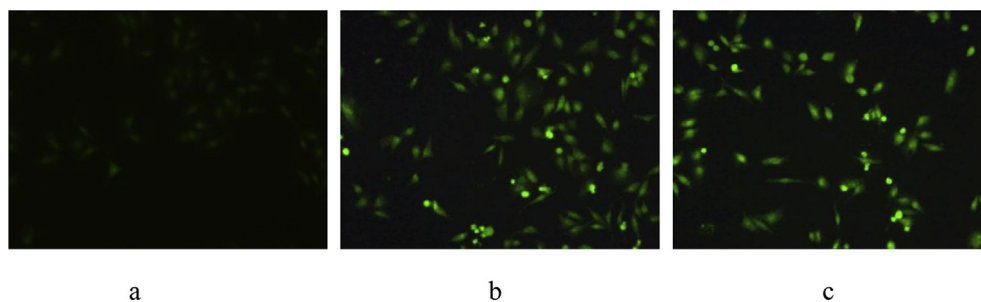


Fig. 4. TUNEL assay of compound **8k** in HeLa cells. (a) Not treated with the **8k** were used as control for 24 h and (b, c) treatment with compound **8k** (15 μ M) for 12 h and 24 h, respectively.

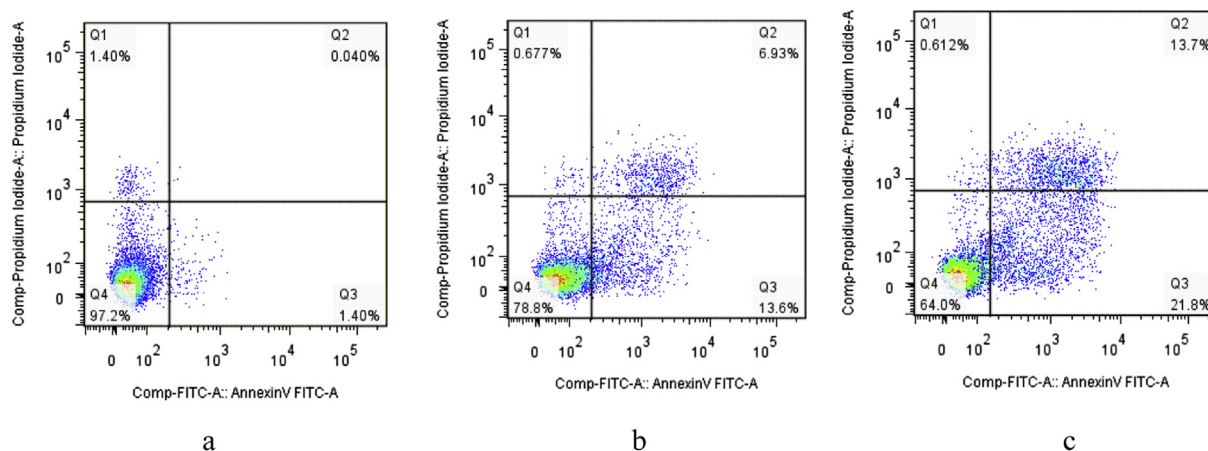


Fig. 5. Apoptosis ratio detection of compound **8k** by Annexin V/PI assay. (a) HeLa cells were not treated with **8k** for 12 h, respectively. (b, c) HeLa cells were treated with compound **8k** at 10 μM and 15 μM for 12 h, respectively.

Hoechst 33258, JC-1 mitochondrial membrane potential staining and TUNEL assay staining under fluorescence microscopy to estimate whether the growth inhibitory activity of the selected compound was related to the induction of apoptosis.

2.3.2. Apoptosis assessment by AO/EB staining

Apoptosis induced by compounds is one of the considerations in drug development. To further address the death pattern, HeLa cells were stained with acridine orange (AO) and ethidium bromide (EB). AO, which is a vital dye, can stain nuclear DNA across an intact cell membrane, while EB can only stain cells that had lost their membrane integrity. Therefore, after synchronous treating with AO and EB, live cells will be evenly stained as green (in the web version) and early apoptotic cells will be thickly stained as green yellow or show green yellow fragments (in the web version), while late apoptotic cells will be densely stained as orange or display orange fragments and necrotic cells will be stained as orange with no condensed chromatin.

The cytotoxicity of compound **8k** at a concentration of 15 μM against HeLa cells from 12 h to 24 h was detected by AO/EB staining, and HeLa cells not treated with the **8k** were used as control for 48 h. The results were shown in Fig. 1. Results depicted in Fig. 1 indicate that control cells did not take up EB and appeared faint orange-red. While cells treated with **8k** at 15 μM showed obvious apoptotic characters (chromatin condensation or fragmentation) and appeared intense orange-red, as dead cells have ruptured membrane which allowed EB to enter into the cells. Also due to the AO uptake, control cells appeared green while **8k** treated cells appeared green to intense green as apoptotic cells have much more permeable membranes. These findings indicate that compound **8k** was able to induce apoptosis.

2.3.3. Apoptosis assessment by Hoechst 33258 staining

Hoechst 33258, which stains the cell nucleus, is a membrane permeable dye with blue fluorescence. Live cells with uniformly light blue nuclei were obviously detected under fluorescence microscope after treatment with Hoechst 33258, whereas apoptotic cells had bright blue nuclei due to karyopyknosis and chromatin condensation. However, the nuclei of dead cells could not be stained. HeLa cells treated with compound **8k** at a concentration of 15 μM from 12 to 24 h were stained with Hoechst 33258. HeLa cells not treated with the **8k** were used as control at for 24 h. The results were given in Fig. 2.

As shown in Fig. 2, cells not treated with compound **8k** were normally blue (in the web version). It was worth noting that, for **8k** treatment, the cells displayed strong blue fluorescence and indicated typical apoptotic morphology after 12 and 24 h. The observation revealed that compounds **8k** induced apoptosis against cell lines, consistent with the results for AO/EB double staining.

2.3.4. Mitochondrial membrane potential staining

In order to further investigate the apoptosis-inducing effect of target compound **8k**, mitochondrial membrane potential ($\Delta\Psi_m$) changes were designed and detected, using the fluorescent probe JC-1. JC-1, which is a lipophilic cationic dye, can easily pass through the plasma membrane into cells and accumulates in actively respiring mitochondria. In the control cells, JC-1 could aggregate in mitochondria and present high red fluorescence. However, in cells undergoing apoptosis, where the mitochondrial potential has collapsed, JC-1 exists in the cytosol as a monomer which emits green fluorescence. HeLa cells treated with compound **8k** at a concentration of 15 μM for 24 h were stained with JC-1 and not treated with the compound **8k** were used as control for 24 h. The results were shown in Fig. 3.

The JC-1 monomer and J-aggregates were excited at 514 nm and 585 nm, respectively, and light emissions were collected at 515–545 nm (green) and 570–600 nm (red). For fluorescence microscopy, Fig. 3 showed that cells not treated with the compound **8k** were normally red (in the web version), while for **8k** treatment, cells showed strong green fluorescence and indicated typical apoptotic morphology after 24 h. Therefore, it could be concluded that compound **8k** induced apoptosis against HeLa cell line. The results were identical with that of previous experiment of AO/EB double staining and Hoechst 33258 staining.

2.3.5. TUNEL assay

TUNEL (terminal-deoxynucleotidyl transferase mediated nick end labeling) is a common method for identifying apoptotic cells in situ by detecting DNA fragmentation. When the genomic DNA is broken, the exposed 3' at the end of deoxynucleotide transfer as the catalytic plus green fluorescent probes fluorescein (FITC) labeled dUTP, which can be detected by fluorescence microscopy or flow cytometry, as indicated by a green color (in the web version). The results were illustrated in Fig. 4.

For fluorescence microscopy, Fig. 4 revealed that HeLa cells treated with the compound **8k** at different time appeared in green (in the web version), indicating that compound **8k** significantly

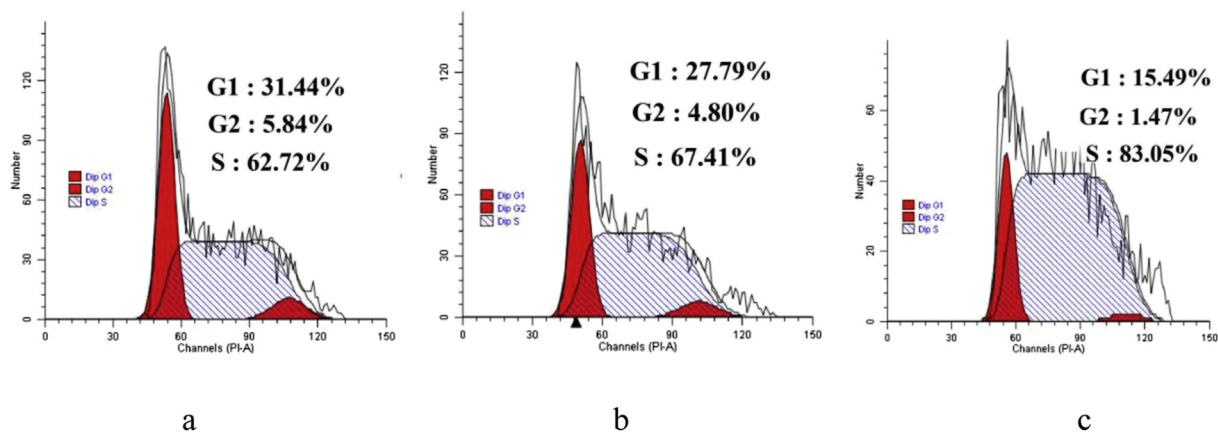


Fig. 6. Investigation of cell cycle distribution by flow cytometric analysis. (a) Untreated HeLa cells as a control. (b, c) Cells was treated with increasing concentrations of compound **8k** (10 and 15 μ M) for 48 h.

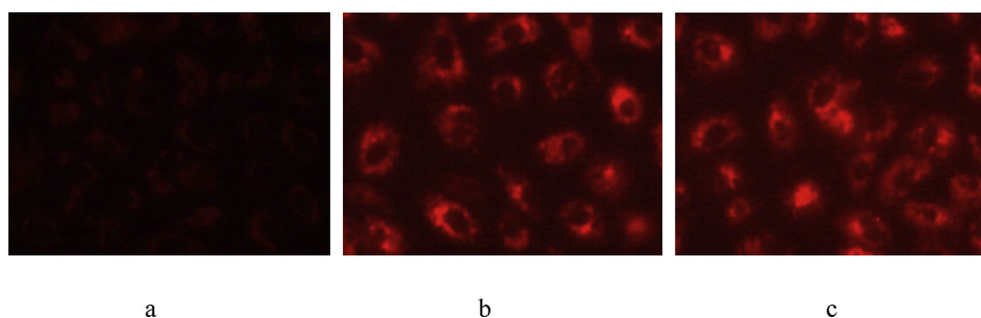


Fig. 7. Induction of cytochrome c release assay of compound **8k** in HeLa cells. (a) Not treated with the **8k** were used as control for 12 h and (b, c) treatment with compound **8k** (10 μ M, 15 μ M) for 12 h, respectively.

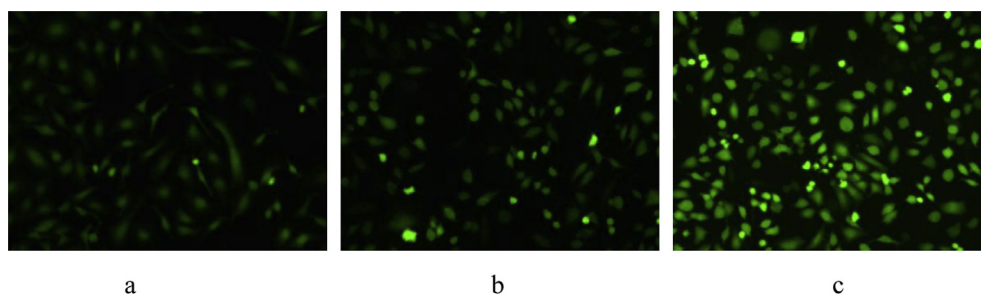


Fig. 8. ROS generation assay of compound **8k** in HeLa cells. (a) Not treated with the **8k** were used as control for 12 h and (b, c) treatment with compound **8k** (10 μ M, 15 μ M) for 12 h, respectively.

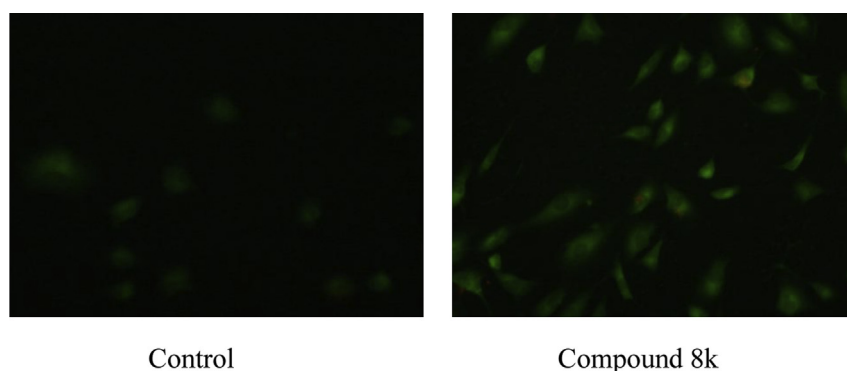


Fig. 9. Activation of Caspase-3 induced by compound **8k**, examined by FITC-DEVD-FMK under a fluorescent microscope.

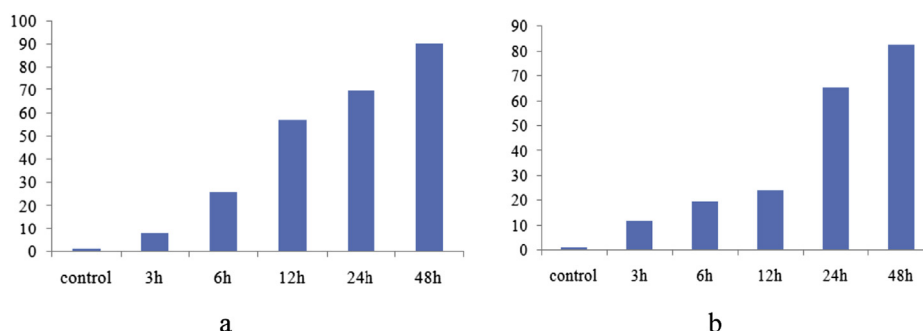


Fig. 10. Measurement of caspase-9 and -3 activities. Dose-dependent induction of caspase-3 in human HeLa cell line.

induced apoptosis against HeLa cell line. The results were consistent well with the previous experiments.

2.4. Apoptosis study by flow cytometry assay

The apoptosis ratios induced by compound **8k** in HeLa tumor cells were quantitatively determined by flow cytometry. Four quadrant images were observed by flow cytometric analysis: the Q1 area represented damaged cells appearing in the process of cell collection, the Q2 region showed necrotic cells and later period apoptotic cells, the Q3 area showed early apoptotic cells, and the normal cells were located in the Q4 area. The results were given in Fig. 5.

Fig. 5 revealed that compound **8k** could induce apoptosis in HeLa cells. Apoptosis ratios (including the early and late apoptosis ratios) for compound **8k** were obtained after 12 h of treatment at the concentration of 10 μ M and 15 μ M. The apoptosis of HeLa cells treated with compound **8k** increased gradually in a concentration manner. The apoptosis ratios of compound **8k** measured at different concentration points were found to 20.53% and 34.5%, respectively, while that of control was 1.44%. The results evidently illustrated that compound **8k** suppressed cell proliferation by inducing apoptosis.

2.5. Investigation of cell cycle distribution

The cell cycle is the series of events that take place in a cell leading to its division and duplication (replication). The cell cycle consists of four distinct phases: G1 phase, S phase (synthesis), G2 phase (collectively known as inter-phase) and M phase (mitosis). The G1 stage is the stage when preparation of energy and material for DNA replication occurs. The S stage is the stage when DNA

replication occurs. The G2 stage is the stage when preparation for the M stage occurs. The M stage is “mitosis”, and is when nuclear and cytoplasmic division occurs. To determine the possible role of cell cycle arrest in DHA derivative-induced growth inhibition, HeLa cells were treated with different concentrations of compound **8k**. Cell cycle distribution was observed by flow cytometric analysis after staining of the DNA with propidium iodide (PI). With an increase of concentration of compound **8k**, the cells accumulated in the S phase cells were gradually increased (Fig. 6), which inferred that compound **8k** arrested HeLa cells in S phase.

2.6. Mechanism of action

2.6.1. Induction of cytochrome c release assay

Activation of apoptotic pathways is a key method by which anti-cancer drugs kill tumor cells [33]. It is well-known that anti-cancer drugs can stimulate apoptotic signaling through two major pathways. Two major pathways described as the extrinsic (death receptor) pathway and the intrinsic (mitochondrial) pathway mediate apoptosis. One is the extrinsic (death receptor) pathway involving in Fas ligand binding to Fas receptors that induces intracellular signaling and the cleavage and activation of caspase-8 [34]. Another apoptotic pathway is the mitochondrial (intrinsic) pathway, which is activated by the release of pro-apoptotic factors from mitochondria inter-membrane space such as cytochrome c [35,36]. Mitochondria play an important role in cell death by changing its outer and inner membrane permeability and thus leading to cytochrome c release and caspases activation [36,44]. Herein, we demonstrated that compound **8k** could disrupt the function of mitochondria at the early stage of apoptosis and subsequently coordinate caspase activation through the release of cytochrome c. HeLa cells treated with different concentrations of compound **8k** for 12 h. The results were shown in Fig. 7.

As shown in Fig. 7, nuclei with karyopyknosis and conglomeration, a characteristic of apoptosis, were observed under fluorescence microscopy in cells cultured with compound **8k**, while the control cells appeared with regular contours. These results showed that compound **8k** was able to induce a loss of mitochondrial trans-membrane potential and release of mitochondrial cytochrome c into the cytosol. Therefore, it could be concluded that the apoptosis induced by compound **8k** in HeLa cells may be through the intrinsic pathway.

2.6.2. ROS generation assay

Recently, oxidative damage to the mitochondrial membrane due to increased generation of ROS has been shown to play a role in apoptosis [37–39]. Mitochondria have also been implicated as a source of ROS during apoptosis. Reduced mitochondria membrane potential has recently been shown to lead to increased generation

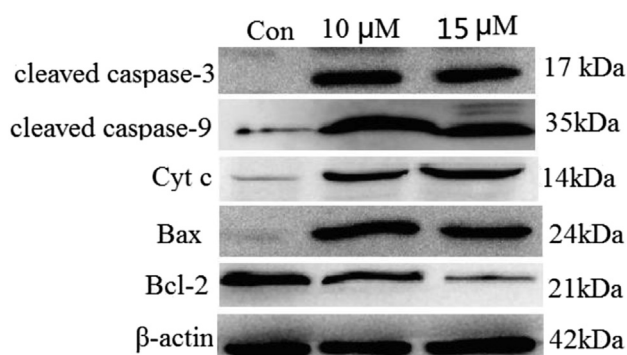


Fig. 11. Western blotting analysis of the levels of Cytochrome c in cytosol, Bax, Bcl-2, caspase-9 and caspase-3 expression in HeLa cells.

of ROS and apoptosis [40]. Furthermore, we studied the loss of mitochondrial trans-membrane potential resulting in the generation of ROS by assessing ROS generation caused by target compound **8k** *in vitro*, using the fluorescent probe 2,7-dichlorofluorescein diacetate (DCF-DA) determined by fluorescence microscopy. Treated with compound **8k** cells exhibited stronger fluorescence intensity in cytoplasm and not treated with compound **8k** cells under the same experimental procedures were used as control and the fluorescence detected in these cells were weak and spread all over the cells.

For fluorescence microscopy, Fig. 8 revealed that HeLa cells treated with the compound **8k** appeared in stronger green fluorescence (in the web version), indicating that compound **8k** significantly induced apoptosis against HeLa cell line. This phenomenon implied that the increment of ROS might play a role as an early mediator in compound **8k** induced apoptosis. These findings pointed to an effect of compound **8k** on mitochondrial function and accumulation of ROS. These features were cues for the induction of apoptosis.

2.6.3. Caspase-3 and -9 activities assay

Apoptosis is an essential cellular process that regulates and maintains the balance between proliferation, growth arrest and cell death. Caspases are a family of cysteinyl aspartate specific proteases involved in apoptosis and are dichotomized to groups of initiators (caspases 8, 9 and 10) and executioners (caspases 3, 6 and 7) [41,42]. Caspase-3 is known as a key executioner caspase in apoptosis and is activated both in the intrinsic and extrinsic apoptotic pathway [43]. Therefore, therapeutic strategies designed to stimulate apoptosis by activating Caspase-3 may help in combating cancer caused by apoptosis deficiency. Thus, we investigated whether the caspase-3 was activated when HeLa cells were exposed to compound **8k**. As shown in Fig. 9, cells treated with compound **8k** had a significant increase in the activity of caspase-3 as indicated by a notable shift in the ratio of green/dark fluorescence versus control. As shown in Fig. 10, the results clearly showed that an induction of cell apoptosis took place when the cells were treated with compound **8k**, and the stimulation of caspase-9 and -3 activities both increased in a time dependent manner from 3 to 48 h.

2.6.4. Western blotting analyses

Apoptosis, a physiological program of cellular death, has a critical role during normal development and in cellular homeostasis. It is well-known that both Fas-dependent and mitochondria-dependent apoptotic pathways are considered major pathways directly causing neuronal apoptosis. Mitochondria play an important role in cell death by changing its outer and inner membrane permeability and thus leading to cytochrome *c* release and caspases activation [44]. To further explore whether compound **8k** induced apoptosis via the mitochondrial signaling pathway, a number of key protein markers involved in mitochondria-mediated apoptosis were also examined by Western blot analysis. Above all, we determined the levels of cytochrome *c* in both mitochondrial and cytosolic fractions, as shown in Fig. 11, compared with the control groups, the level of cytochrome *c* in cytosol was increased after treatment with **8k** for 24 h. Cytochrome *c* is reportedly involved in the activation of the downstream caspases that trigger apoptosis [45]. In addition, we examined the roles of caspase-9 and caspase-3 in the cellular response to compound **8k**. As shown in Fig. 11, western blot analysis showed that treatment of HeLa cells with compound **8k** significantly increased to cleavage of caspase-9 and caspase-3.

The Bcl-2 family members are important regulators of the mitochondrial apoptotic pathway. Two most important members of

Bcl-2 family, the anti-apoptotic protein Bcl-2 and the pro-apoptotic protein Bax, are key regulators of this progress [46]. In order to clarify the mechanism of compound **8k** induced in HeLa cells apoptosis, this study investigated the expression of Bax and Bcl-2 proteins. As shown in Fig. 11, western blotting testing revealed that elevation of Bax expression, compared with control group, whereas the protein expression level of Bcl-2 was decreased in a dose-dependent manner. Taken together, our results suggest that compound **8k** may induce tumor apoptosis through mitochondrial death pathways.

3. Conclusions

In the present study, a series of novel DHA chiral dipeptide derivatives were designed and synthesized. Cytotoxicity assay of target compounds against HeLa, NCI-H460 and MGC-803 cells showed that compound **8k** exhibited the highest cytotoxicity against HeLa cell line. The apoptosis-inducing activity of representative compound **8k** in HeLa cells were investigated by AO/EB staining, Hoechst 33258 staining, JC-1 mitochondrial membrane potential staining, TUNEL assay and flow cytometry. Furthermore, compound **8k** was found to induce apoptosis in HeLa cells via the mitochondrial pathway, the underlying mechanisms for the anticancer activity were associated with loss of mitochondrial membrane potential, enhancement of mitochondrial cytochrome *c* release and intracellular ROS production, elevation of Bax expression, down-regulation of Bcl-2, and the activation of caspase-9 and -3. In this paper, these findings may open a new door for the design and synthesis of new anticancer drugs, and DHA derivative might be a promising lead compound suitable for developing new drug as anticancer therapy.

4. Experimental

4.1. General

Compound **2** was synthesized according to the literature [17]. Compound **6** was synthesized according to the literature [17]. All the chemical reagents and solvents used were of analytical grade. Silica gel (200–300 mesh) used in column chromatography was provided by Tsingtao Marine Chemistry Co. Ltd. ^1H NMR spectra were recorded on a BRUKER AV-400 spectrometer with TMS as an internal standard in CDCl_3 . Mass spectra were determined on an FTMS ESI spectrometer.

4.2. Synthesis: general procedure for compounds **8a–8p**

Compound **2** (1 mmol) added to dry CH_2Cl_2 (15 mL) was stirred at 0 °C and oxalyl chloride (1.5 mmol) was dripped into the mixture and stirred at room temperature for 6 h. After the reaction, the solvent and excess oxalyl chloride was evaporated under reduced pressure. Aromatic primary amines (1 mmol) and triethylamine (0.5 mmol) were added to the mixture and stirred at room temperature for 0.5 h. After the reaction, the solvent was evaporated under reduced pressure, and the crude product was purified by chromatography on silica gel eluted with petroleum ether/ethyl acetate (V: V = 6:1) to offer compound **4**. Compound **4** (1 mmol) and hydrazine hydrate (3 mmol) were added to ethanol (15 mL) and the mixture was stirred at room temperature for 8 h. After the reaction was completed, the solvent was evaporated under reduced pressure, and the crude product was purified by chromatography on silica gel eluted with petroleum ether/ethyl acetate (V: V = 3: 1) to obtain compounds **5**. compounds **6** (1 mmol) added to dry CH_2Cl_2 (15 mL) was stirred at 0 °C and oxalyl chloride (1.5 mmol) was dripped into the mixture and stirred at room temperature for

6 h. After the reaction, the solvent and excess oxalyl chloride was evaporated under reduced pressure. Compounds **5** (1 mmol) and triethylamine (0.5 mmol) were added to the mixture and stirred at room temperature for 0.5 h. After the reaction, the solvent was evaporated under reduced pressure, and the crude product was purified by chromatography on silica gel eluted with petroleum ether/ethyl acetate (V: V = 6:1) to offer compounds **8a–8p**. The structures were confirmed by ^1H NMR, ^{13}C NMR and HR-MS (see Supporting information).

Compound 8a: Yields 87.5%; ^1H NMR (400 MHz, CDCl_3): δ 8.54 (s, 1H, NH), 7.84 (d, J = 2.1 Hz, 1H), 7.40 (dd, J = 8.2, 2.1 Hz, 1H), 7.33 (d, J = 1.1 Hz, 1H), 7.30 (t, J = 2.0 Hz, 1H), 7.27 (dd, J = 5.2, 2.1 Hz, 2H), 7.25 (s, 1H), 7.24–7.21 (m, 3H), 7.19 (s, 1H), 7.05 (d, J = 7.3 Hz, 1H), 6.78 (d, J = 7.5 Hz, 1H), 4.93–4.87 (m, 1H), 3.17 (d, J = 7.2 Hz, 2H), 2.95–2.90 (m, 1H), 2.72–2.50 (m, 2H), 2.31 (d, J = 12.9 Hz, 1H), 2.20–2.14 (m, 1H), 1.77–1.57 (m, 5H), 1.30 (s, 3H, CH_3), 1.25 (d, J = 2.9 Hz, 6H, $2 \times \text{CH}_3$), 1.23 (s, 3H, CH_3). ^{13}C NMR (100 MHz, CDCl_3): δ 198.25, 177.87, 169.45, 152.93, 146.89, 137.30, 136.29, 132.52, 130.72, 129.27, 128.86, 128.80, 127.31, 125.05, 124.45, 123.27, 120.21, 55.40, 46.39, 43.39, 38.43, 37.20, 36.81, 33.54, 23.84, 23.77, 23.75, 18.09, 16.24. HR-MS (m/z) (ESI): calcd for $\text{C}_{35}\text{H}_{40}\text{N}_2\text{O}_3$ [$\text{M}+\text{H}^+$]: 537.31172; found: 537.31329.

Compound 8b: Yields 82%; ^1H NMR (400 MHz, CDCl_3): δ 8.40 (s, 1H, NH), 7.86 (d, J = 2.0 Hz, 1H), 7.43–7.41 (m, 1H), 7.35 (d, J = 8.0 Hz, 2H), 7.28 (s, 2H), 7.22 (s, 3H), 7.19 (s, 2H), 7.06 (s, 1H), 6.70 (d, J = 7.3 Hz, 1H), 4.90–4.851 (m, 1H), 3.14 (d, J = 7.0 Hz, 2H), 2.98–2.93 (m, 1H), 2.64–2.61 (m, 2H), 2.34 (d, J = 7.9 Hz, 1H), 2.33–2.30 (m, 1H), 1.78–1.53 (m, 5H), 1.32 (s, 3H, CH_3), 1.28 (s, 3H, CH_3), 1.26 (d, J = 6.7 Hz, 6H, $2 \times \text{CH}_3$). ^{13}C NMR (100 MHz, CDCl_3): δ 198.09, 177.78, 169.28, 152.90, 146.93, 137.31, 136.47, 132.51, 130.78, 129.27, 128.88, 128.72, 127.15, 125.11, 124.46, 123.29, 120.11, 55.35, 46.51, 44.08, 38.26, 37.37, 37.28, 37.09, 37.02, 33.62, 23.86, 23.77, 18.28, 16.20. HR-MS (m/z) (ESI): calcd for $\text{C}_{35}\text{H}_{40}\text{N}_2\text{O}_3$ [$\text{M}+\text{H}^+$]: 537.31172; found: 537.31335.

Compound 8c: Yields 85%; ^1H NMR (400 MHz, CDCl_3): δ 8.30 (s, 1H, NH), 8.07–7.81 (m, 2H), 7.40 (d, J = 1.6 Hz, 1H), 7.31 (d, J = 19.0 Hz, 4H), 7.23 (d, J = 5.9 Hz, 1H), 7.00 (d, J = 39.0 Hz, 2H), 6.83 (d, J = 6.6 Hz, 1H), 6.57 (s, 1H), 4.87–4.77 (m, 1H), 3.73 (s, 3H, OCH_3), 3.27–3.11 (m, 2H), 2.93 (d, J = 5.9 Hz, 1H), 2.78–2.50 (m, 2H), 2.35 (d, J = 12.1 Hz, 1H), 2.21 (d, J = 18.0 Hz, 1H), 1.81–1.61 (m, 5H), 1.33 (s, 3H, CH_3), 1.26–1.20 (m, 9H, $3 \times \text{CH}_3$). ^{13}C NMR (100 MHz, CDCl_3): δ 198.39, 177.12, 168.88, 152.94, 148.02, 146.88, 136.42, 132.43, 130.89, 129.28, 128.84, 128.67, 127.21, 125.03, 124.13, 123.21, 120.9, 119.77, 109.91, 55.60, 55.55, 46.40, 43.48, 38.62, 37.22, 37.16, 37.11, 36.96, 33.60, 23.84, 23.77, 18.27, 16.35. HR-MS (m/z) (ESI): calcd for $\text{C}_{36}\text{H}_{42}\text{N}_2\text{O}_4$ [$\text{M}+\text{H}^+$]: 567.32228; found: 567.31983.

Compound 8d: Yields 85.52%; ^1H NMR (400 MHz, CDCl_3): δ 8.31 (s, 1H, NH), 8.04 (s, 1H, NH), 7.85 (d, J = 1.9 Hz, 1H), 7.42 (dd, J = 8.1, 1.9 Hz, 1H), 7.30 (s, 1H), 7.28 (d, J = 1.6 Hz, 1H), 7.26 (s, 1H), 7.23 (d, J = 4.9 Hz, 2H), 7.21 (d, J = 4.1 Hz, 1H), 7.06 (d, J = 7.5 Hz, 1H), 6.97 (d, J = 7.7 Hz, 1H), 6.86 (d, J = 8.1 Hz, 1H), 6.54 (d, J = 7.2 Hz, 1H), 4.86–4.81 (m, 1H), 3.77 (s, 3H, OCH_3), 3.21–3.11 (m, 2H), 2.98–2.91 (m, 1H), 2.71–2.56 (m, 2H), 2.36 (d, J = 14.9 Hz, 2H), 1.79–1.58 (m, 5H), 1.33 (s, 3H, CH_3), 1.29 (d, J = 6.6 Hz, 6H, $2 \times \text{CH}_3$), 1.26 (s, 3H, CH_3). ^{13}C NMR (100 MHz, CDCl_3): δ 198.30, 177.12, 168.78, 153.05, 148.07, 146.92, 136.44, 132.45, 130.89, 129.32, 128.69, 127.04, 127.96, 125.03, 124.15, 123.25, 120.85, 119.82, 109.98, 55.66, 55.32, 46.36, 43.78, 38.29, 37.31, 37.23, 37.16, 37.00, 33.61, 23.86, 23.79, 18.32, 16.37. HR-MS (m/z) (ESI): calcd for $\text{C}_{36}\text{H}_{42}\text{N}_2\text{O}_4$ [$\text{M}+\text{H}^+$]: 567.32228; found: 567.31995.

Compound 8e: Yields 86.58%; ^1H NMR (400 MHz, CDCl_3): δ 8.10 (s, 1H, NH), 7.86 (s, 1H, NH), 7.41 (d, J = 8.1 Hz, 1H), 7.32 (d, J = 6.6 Hz, 2H), 7.29 (s, 3H), 7.24 (s, 1H), 7.21 (d, J = 7.2 Hz, 2H), 6.77–6.74 (m, 2H), 6.68 (d, J = 7.1 Hz, 1H), 4.86–4.81 (m, 1H), 3.77 (s, 3H, OCH_3), 3.22–3.12 (m, 2H), 2.96–2.91 (m, 1H), 2.75–2.51 (m,

2H), 2.33 (d, J = 12.2 Hz, 1H), 2.20 (d, J = 16.9 Hz, 1H), 1.83–1.60 (m, 5H), 1.31 (s, 3H, CH_3), 1.27 (s, 3H, CH_3), 1.25 (d, J = 2.6 Hz, 6H, $2 \times \text{CH}_3$). ^{13}C NMR (100 MHz, CDCl_3): δ 198.27, 177.69, 169.05, 156.55, 152.96, 146.93, 136.46, 132.50, 130.81, 130.33, 129.31, 128.91, 127.32, 125.07, 123.27, 121.98, 114.02, 55.44, 55.40, 46.40, 43.54, 38.51, 37.22, 37.17, 37.12, 36.93, 33.60, 23.83, 23.75, 18.20, 16.33. HR-MS (m/z) (ESI): calcd for $\text{C}_{36}\text{H}_{42}\text{N}_2\text{O}_4$ [$\text{M}+\text{H}^+$]: 567.32228; found: 567.31985.

Compound 8f: Yields 84.25%; ^1H NMR (400 MHz, CDCl_3): δ 7.99 (s, 1H, NH), 7.86 (d, J = 1.6 Hz, 1H), 7.43–7.40 (m, 1H), 7.28 (s, 1H), 7.26 (d, J = 2.8 Hz, 2H), 7.22 (d, J = 7.23 Hz, 3H), 6.79 (d, J = 8.9 Hz, 3H), 6.65 (d, J = 7.0 Hz, 1H), 4.83–4.77 (m, 1H), 3.79 (s, 3H, OCH_3), 3.14 (dd, J = 10.5, 7.3 Hz, 2H), 2.97–2.92 (m, 1H), 2.68–2.57 (m, 2H), 2.32 (dd, J = 10.1, 3.9 Hz, 2H), 1.76–1.53 (m, 5H), 1.32 (s, 3H, CH_3), 1.28 (s, 3H, CH_3), 1.26 (s, 3H, CH_3), 1.25 (s, 3H, CH_3). ^{13}C NMR (100 MHz, CDCl_3): δ 198.16, 177.62, 168.97, 156.65, 152.77, 147.01, 136.58, 132.50, 130.78, 130.28, 129.29, 128.75, 127.14, 125.09, 123.30, 121.96, 114.09, 55.45, 55.32, 46.50, 44.06, 38.29, 37.40, 37.29, 37.06, 37.02, 33.61, 23.85, 23.76, 18.28, 16.26. HR-MS (m/z) (ESI): calcd for $\text{C}_{36}\text{H}_{42}\text{N}_2\text{O}_4$ [$\text{M}+\text{H}^+$]: 567.32228; found: 567.32124.

Compound 8g: Yields 82.45%; ^1H NMR (400 MHz, CDCl_3): δ 8.28 (s, 1H, NH), 7.86 (d, J = 1.9 Hz, 1H), 7.41 (dd, J = 8.2, 1.9 Hz, 1H), 7.33 (d, J = 5.5 Hz, 2H), 7.29 (d, J = 4.9 Hz, 1H), 7.26 (d, J = 6.1 Hz, 3H), 7.22 (d, J = 8.1 Hz, 2H), 7.08 (d, J = 7.5 Hz, 1H), 6.70 (d, J = 7.4 Hz, 1H), 4.88–4.83 (m, 1H), 3.22–3.14 (m, 2H), 2.95 (d, J = 6.9 Hz, 1H), 2.76–2.54 (m, 2H), 2.33 (d, J = 12.8 Hz, 1H), 2.20–2.15 (m, 1H), 1.76–1.58 (m, 5H), 1.31 (s, 3H, CH_3), 1.27 (s, 3H, CH_3), 1.25 (d, J = 4.4 Hz, 6H, $2 \times \text{CH}_3$). ^{13}C NMR (101 MHz, CDCl_3): δ 198.27, 177.87, 169.31, 152.95, 146.93, 137.29, 136.37, 132.52, 130.80, 129.28, 128.95, 128.86, 127.37, 125.08, 124.50, 123.27, 120.17, 55.52, 46.44, 43.50, 38.30, 37.20, 37.17, 37.14, 36.92, 33.60, 23.84, 23.76, 18.20, 16.33. HR-MS (m/z) (ESI): calcd for $\text{C}_{35}\text{H}_{39}\text{N}_2\text{O}_3\text{F}$ [$\text{M}+\text{H}^+$]: 555.30230; found: 555.30152.

Compound 8h: Yields 83.25%; ^1H NMR (400 MHz, CDCl_3): δ 8.26 (s, 1H, NH), 8.19 (dd, J = 11.3, 4.4 Hz, 1H), 7.85 (dd, J = 6.4, 2.0 Hz, 1H), 7.43–7.39 (m, 1H), 7.35 (d, J = 7.5 Hz, 1H), 7.29 (d, J = 3.0 Hz, 1H), 7.27 (dd, J = 5.1, 1.9 Hz, 1H), 7.20 (dd, J = 8.5, 5.6 Hz, 2H), 7.13–7.01 (m, 3H), 6.51 (t, J = 7.4 Hz, 1H), 4.91–4.87 (m, 1H), 3.24–3.10 (m, 2H), 2.94 (dd, J = 13.8, 6.9 Hz, 1H), 2.77–2.47 (m, 2H), 2.37–2.08 (m, 2H), 1.79–1.52 (m, 5H), 1.31 (s, 3H, CH_3), 1.28 (s, 3H, CH_3), 1.27 (s, 3H, CH_3), 1.24 (s, 3H, CH_3). ^{13}C NMR (100 MHz, CDCl_3): δ 198.20, 177.69, 169.51, 152.83, 146.91, 136.19, 132.42, 130.85, 129.14, 129.02, 128.78, 127.42, 127.22, 125.08, 124.40, 123.20, 122.12, 115.10, 55.19, 46.47, 43.93, 43.31, 37.72, 37.23, 37.09, 36.96, 36.68, 33.59, 23.86, 23.77, 18.26, 16.29. HR-MS (m/z) (ESI): calcd for $\text{C}_{35}\text{H}_{39}\text{N}_2\text{O}_3\text{F}$ [$\text{M}+\text{H}^+$]: 555.30230; found: 555.30371.

Compound 8i: Yields 81.52%; ^1H NMR (400 MHz, CDCl_3): δ 8.39 (s, 1H, NH), 7.86 (d, J = 2.0 Hz, 1H), 7.43 (dd, J = 8.1, 2.0 Hz, 1H), 7.33 (s, 1H), 7.31 (s, 1H), 7.29 (d, J = 1.7 Hz, 2H), 7.26 (dd, J = 4.1, 1.8 Hz, 2H), 7.23 (d, J = 6.4 Hz, 2H), 6.91–6.86 (m, 2H), 6.63 (d, J = 7.3 Hz, 1H), 4.87–4.82 (m, 1H), 3.18 (dd, J = 7.2, 3.4 Hz, 2H), 2.98–2.92 (m, 1H), 2.74–2.53 (m, 2H), 2.34 (d, J = 11.5 Hz, 1H), 2.18 (dd, J = 18.0, 3.5 Hz, 1H), 1.77–1.60 (m, 5H), 1.31 (s, 3H, CH_3), 1.28 (s, 3H, CH_3), 1.25 (d, J = 2.0 Hz, 6H, $2 \times \text{CH}_3$). ^{13}C NMR (100 MHz, CDCl_3): δ 198.16, 177.95, 169.21, 160.64, 158.22, 152.91, 147.02, 136.24, 133.30, 132.59, 130.74, 129.25, 128.96, 127.41, 125.08, 123.30, 121.97, 121.89, 115.58, 115.35, 55.43, 46.45, 43.56, 38.36, 37.23, 37.20, 37.18, 33.60, 23.81, 23.75, 23.73, 18.18, 16.33. HR-MS (m/z) (ESI): calcd for $\text{C}_{35}\text{H}_{39}\text{N}_2\text{O}_3\text{F}$ [$\text{M}+\text{H}^+$]: 555.30230; found: 555.30477.

Compound 8j: Yields 83.54%; ^1H NMR (400 MHz, CDCl_3): δ 8.64 (s, 1H, NH), 7.86 (d, J = 2.0 Hz, 1H), 7.43 (dd, J = 8.2, 2.0 Hz, 1H), 7.27 (dd, J = 6.9, 2.2 Hz, 3H), 7.22 (d, J = 7.3 Hz, 2H), 7.17 (dd, J = 6.6, 5.1 Hz, 2H), 6.87 (t, J = 8.7 Hz, 2H), 6.67 (d, J = 7.3 Hz, 1H), 4.90–4.85 (m, 1H), 3.17–3.10 (m, 2H), 2.96 (dd, J = 13.8, 6.9 Hz, 1H), 2.67–2.57 (m, 2H), 2.34 (t, J = 11.5 Hz, 2H), 1.77–1.49 (m, 5H), 1.32 (s, 3H, CH_3),

1.28 (s, 3H, CH₃), 1.27 (s, 3H, CH₃), 1.25 (s, 3H, CH₃). ¹³C NMR (100 MHz, CDCl₃) δ 197.99, 178.00, 169.20, 160.57, 158.15, 152.83, 147.00, 136.35, 133.37, 132.57, 130.67, 129.19, 128.71, 125.10, 123.31, 121.78, 121.70, 115.55, 115.32, 55.36, 46.56, 44.15, 38.20, 37.37, 37.28, 37.01, 33.59, 23.82, 23.73, 18.25, 16.23. HR-MS (*m/z*) (ESI): calcd for C₃₅H₃₉N₂O₃F [M+H⁺]: 555.30230; found: 555.30419.

Compound **8k**: Yields 82.54%; ¹H NMR (400 MHz, CDCl₃): δ 8.19 (s, 1H, NH), 7.86 (d, *J* = 2.0 Hz, 1H), 7.35 (dd, *J* = 8.0, 1.2 Hz, 2H), 7.29 (d, *J* = 1.5 Hz, 2H), 7.28–7.25 (m, 3H), 7.22 (d, *J* = 4.4 Hz, 2H), 7.20–7.15 (m, 1H), 7.08–7.04 (m, 1H), 4.89–4.84 (m, 1H), 3.23–3.18 (m, 2H), 2.97–2.92 (m, 1H), 2.63–2.56 (m, 2H), 2.36–2.29 (m, 2H), 1.77–1.60 (m, 5H), 1.32 (s, 3H, CH₃), 1.28 (s, 3H, CH₃), 1.27 (s, 3H, CH₃), 1.24 (s, 3H, CH₃). ¹³C NMR (100 MHz, CDCl₃) δ 198.11, 177.56, 169.32, 152.83, 146.94, 136.15, 134.10, 132.45, 130.87, 129.16, 128.88, 127.58, 127.30, 125.11, 123.21, 121.82, 55.35, 46.48, 43.89, 37.78, 37.33, 37.23, 37.14, 36.97, 33.62, 23.86, 23.80, 18.28, 16.36. HR-MS (*m/z*) (ESI): calcd for C₃₅H₃₉N₂O₃Cl [M+H⁺]: 571.27275; found: 571.27423.

Compound **8l**: yields 81.45%; ¹H NMR (400 MHz, CDCl₃) δ 8.21 (s, 1H, NH), 7.86 (d, *J* = 2.0 Hz, 1H), 7.42 (dd, *J* = 8.1, 2.0 Hz, 1H), 7.35 (dd, *J* = 8.1, 1.3 Hz, 2H), 7.26 (dd, *J* = 11.3, 4.3 Hz, 4H), 7.22 (d, *J* = 3.8 Hz, 2H), 7.05 (dd, *J* = 7.7, 1.2 Hz, 1H), 6.44 (d, *J* = 7.1 Hz, 1H), 4.90–4.84 (m, 1H), 3.19 (dd, *J* = 7.1, 3.5 Hz, 2H), 2.94 (dd, *J* = 13.9, 6.9 Hz, 1H), 2.63–2.56 (m, 2H), 2.36–2.29 (m, 2H), 1.76–1.52 (m, 5H), 1.32 (s, 3H, CH₃), 1.28 (s, 3H, CH₃), 1.27 (s, 3H, CH₃), 1.24 (s, 3H, CH₃). ¹³C NMR (100 MHz, CDCl₃) δ 198.14, 177.58, 169.34, 152.84, 146.94, 136.15, 134.09, 132.46, 130.86, 129.16, 128.87, 127.57, 127.29, 125.10, 123.21, 121.85, 55.35, 46.48, 43.89, 37.78, 37.33, 37.23, 37.12, 36.97, 33.61, 23.86, 23.80, 18.28, 16.36. HR-MS (*m/z*) (ESI): calcd for C₃₅H₃₉N₂O₃Cl [M+H⁺]: 571.27275; found: 571.27535.

Compound **8m**: Yields 83.5%; ¹H NMR (400 MHz, CDCl₃): δ 8.62 (s, 1H, NH), 7.87 (s, 1H, NH), 7.43 (d, *J* = 8.1 Hz, 1H), 7.32–7.25 (m, 4H), 7.21 (d, *J* = 7.4 Hz, 2H), 7.13 (d, *J* = 8.6 Hz, 3H), 7.09–7.04 (m, 1H), 6.69 (d, *J* = 7.4 Hz, 1H), 4.91–4.85 (m, 1H), 3.16 (d, *J* = 7.2 Hz, 2H), 2.98–2.93 (m, 1H), 2.65 (d, *J* = 45.1 Hz, 2H), 2.34 (d, *J* = 11.5 Hz, 1H), 2.21–2.15 (m, 1H), 1.77–1.51 (m, 5H), 1.32 (s, 3H, CH₃), 1.28 (s, 3H, CH₃), 1.26 (d, *J* = 1.8 Hz, 6H, 2 × CH₃). ¹³C NMR (100 MHz, CDCl₃) δ 198.12, 178.05, 169.38, 152.90, 147.04, 136.12, 135.93, 132.65, 130.71, 129.41, 129.22, 128.94, 128.81, 127.42, 125.10, 123.31, 121.37, 55.50, 46.49, 43.53, 38.46, 37.32, 37.24, 37.17, 36.91, 36.91, 33.59, 23.82, 23.74, 18.18, 16.33. HR-MS (*m/z*) (ESI): calcd for C₃₅H₃₉N₂O₃Cl [M+H⁺]: 571.27275; found: 571.27486.

Compound **8n**: Yields 81%; ¹H NMR (400 MHz, CDCl₃) δ 8.77 (s, 1H, NH), 7.86 (s, 1H, NH), 7.43 (d, *J* = 8.1 Hz, 1H), 7.29–7.24 (m, 4H), 7.20 (d, *J* = 7.5 Hz, 2H), 7.16–7.12 (m, 4H), 6.68 (d, *J* = 7.2 Hz, 1H), 4.92–4.86 (m, 1H), 3.14–3.05 (m, 2H), 2.99–2.93 (m, 1H), 2.69–2.57 (m, 2H), 2.32 (d, *J* = 15.7 Hz, 2H), 1.76–1.53 (m, 5H), 1.33 (s, 3H, CH₃), 1.29 (s, 3H, CH₃), 1.27 (s, 3H, CH₃), 1.26 (s, 3H, CH₃). ¹³C NMR (100 MHz, CDCl₃) δ 197.92, 178.07, 169.31, 152.78, 147.01, 136.26, 135.99, 132.59, 130.66, 129.15, 128.80, 128.70, 127.17, 125.12, 123.30, 121.48, 121.12, 55.41, 46.56, 44.17, 38.24, 37.39, 37.28, 37.05, 37.01, 33.59, 23.84, 23.73, 18.25, 16.26. HR-MS (*m/z*) (ESI): calcd for C₃₅H₃₉N₂O₃Cl [M+H⁺]: 569.25710; found: 569.25586.

Compound **8o**: Yields 82.45%; ¹H NMR (400 MHz, CDCl₃): δ 8.40 (s, 1H, NH), 7.83 (s, 1H, NH), 7.40 (d, *J* = 8.0 Hz, 1H), 7.32 (d, *J* = 7.2 Hz, 2H), 7.27 (d, *J* = 8.5 Hz, 2H), 7.23 (d, *J* = 7.1 Hz, 2H), 6.62–6.53 (m, 3H), 4.83–4.78 (m, 1H), 3.78 (s, 9H, 3 × OCH₃), 3.16 (d, *J* = 7.3 Hz, 2H), 2.94–2.89 (m, 1H), 2.67–2.48 (m, 2H), 2.34 (d, *J* = 12.0 Hz, 2H), 1.83–1.59 (m, 5H), 1.29 (s, 3H, CH₃), 1.25 (d, *J* = 1.26 Hz, 6H, 2 × CH₃), 1.24 (s, 3H, CH₃). ¹³C NMR (100 MHz, CDCl₃) δ 198.13, 178.12, 169.31, 153.10, 152.87, 146.98, 136.33, 134.70, 133.50, 132.58, 130.73, 129.13, 129.05, 127.39, 125.03, 123.30, 97.66, 60.89, 56.02, 55.63, 46.44, 43.71, 38.03, 37.20, 37.12, 37.05, 36.93, 33.57, 23.81, 23.72, 18.20, 16.29. HR-MS (*m/z*) (ESI): calcd for C₃₈H₄₇N₂O₆ [M+H⁺]: 627.34341; found: 627.34239.

Compound **8p**: Yields 84.5%; ¹H NMR (400 MHz, CDCl₃): δ 8.28 (s, 1H, NH), 7.84 (s, 1H, NH), 7.42 (d, *J* = 8.0 Hz, 1H), 7.28–7.21 (m, 7H), 6.65 (s, 2H), 6.53 (d, *J* = 6.1 Hz, 1H), 4.80–4.72 (m, 1H), 3.80 (s, 9H, 3 × OCH₃), 3.15 (d, *J* = 6.9 Hz, 2H), 2.98–2.89 (m, 1H), 2.69–2.55 (m, 2H), 2.35 (d, *J* = 15.1 Hz, 2H), 1.85–1.48 (m, 5H), 1.30 (s, 3H, CH₃), 1.28 (s, 3H, CH₃), 1.26 (s, 3H, CH₃), 1.25 (s, 3H, CH₃). ¹³C NMR (100 MHz, CDCl₃) δ 198.05, 178.03, 169.10, 153.14, 152.85, 147.02, 136.49, 134.70, 133.44, 132.58, 130.72, 129.14, 128.88, 127.21, 125.03, 123.32, 97.62, 60.91, 56.03, 55.56, 46.51, 44.18, 37.76, 37.33, 37.27, 36.97, 36.91, 33.60, 23.85, 23.75, 18.23, 16.26. HR-MS (*m/z*) (ESI): calcd for C₃₈H₄₇N₂O₆ [M+H⁺]: 627.34341; found: 627.34263.

4.3. General procedure for compounds **9a–9p**

Compounds **8** (1 mmol) and hydroxylamine hydrochloride were added to ethanol (15 mL) and the mixture was stirred at 80 °C for 8 h. After the reaction was completed, the solvent was evaporated under reduced pressure, and the crude product was purified by chromatography on silica gel eluted with petroleum ether/ethyl acetate (V:V = 4:1) to obtain compounds **9**. The structures were confirmed by ¹H NMR, ¹³C NMR and HR-MS (see Supporting information).

Compound **9a**: Yields 85%; ¹H NMR (400 MHz, CDCl₃): δ 8.68 (s, 1H, NH), 7.68 (s, 1H, NH), 7.31 (t, *J* = 12.5 Hz, 3H), 7.23–7.20 (m, 4H), 7.17 (d, *J* = 7.7 Hz, 2H), 7.11–7.03 (m, 3H), 6.82 (d, *J* = 7.4 Hz, 1H), 5.00–4.96 (m, 1H), 3.21–3.14 (m, 2H), 2.83–2.72 (m, 2H), 2.67–2.62 (m, 1H), 2.38 (dd, *J* = 13.3, 4.9 Hz, 1H), 2.27 (d, *J* = 11.2 Hz, 1H), 1.62 (dd, *J* = 41.6, 22.0 Hz, 5H), 1.36 (s, 3H, CH₃), 1.20 (s, 3H, CH₃), 1.19 (s, 3H, CH₃), 1.13 (s, 3H, CH₃). ¹³C NMR (100 MHz, CDCl₃): δ 178.29, 169.51, 155.69, 148.74, 146.56, 137.37, 136.23, 129.40, 128.77, 128.68, 128.43, 128.01, 127.10, 124.40, 122.86, 122.28, 120.33, 55.33, 46.47, 41.82, 38.55, 37.47, 37.06, 36.58, 33.66, 24.01, 23.76, 23.75, 23.56, 23.02, 18.19, 16.43. HR-MS (*m/z*) (ESI): calcd for C₃₅H₄₁N₃O₃ [M+H⁺]: 552.32262; found: 552.31995.

Compound **9b**: Yields 83.5%; ¹H NMR (400 MHz, CDCl₃): δ 8.76 (s, 1H, NH), 7.65 (s, 1H, NH), 7.31 (d, *J* = 7.6 Hz, 2H), 7.22–7.19 (m, 4H), 7.17–7.09 (m, 4H), 6.99 (t, *J* = 7.4 Hz, 1H), 6.71 (d, *J* = 7.5 Hz, 1H), 4.99–4.93 (m, 1H), 3.25–3.12 (m, 2H), 2.85–2.78 (m, 1H), 2.63–2.55 (m, 2H), 2.28–2.15 (m, 2H), 1.71–1.45 (m, 5H), 1.29 (s, 3H, CH₃), 1.19 (s, 3H, CH₃), 1.18 (s, 3H, CH₃), 1.07 (s, 3H, CH₃). ¹³C NMR (100 MHz, CDCl₃): δ 178.50, 169.45, 155.43, 148.54, 146.50, 137.38, 136.44, 129.22, 128.74, 128.70, 127.86, 127.12, 124.34, 122.78, 122.21, 120.21, 55.26, 46.52, 42.34, 37.85, 37.44, 37.12, 36.62, 33.66, 24.02, 23.76, 23.34, 22.98, 18.23, 16.32. HR-MS (*m/z*) (ESI): calcd for C₃₅H₄₁N₃O₃ [M+H⁺]: 552.32262; found: 552.32056.

Compound **9c**: Yields 82.25%; ¹H NMR (400 MHz, CDCl₃): δ 7.96 (s, 1H, NH), 7.66 (s, 1H, NH), 7.31–7.25 (m, 4H), 7.23–7.17 (m, 4H), 7.06–7.16.927 (m, 2H), 6.81 (dd, *J* = 8.1, 1.0 Hz, 1H), 6.61 (d, *J* = 7.4 Hz, 1H), 4.89–4.85 (m, 1H), 3.71 (s, 3H, OCH₃), 3.34–3.29 (m, 1H), 3.18–3.09 (m, 2H), 2.84 (d, *J* = 6.9 Hz, 1H), 2.69–2.60 (m, 2H), 2.38–2.33 (m, 1H), 1.74–1.60 (m, 5H), 1.35 (s, 3H, CH₃), 1.22 (s, 3H, CH₃), 1.20 (s, 3H, CH₃), 1.13 (s, 3H, CH₃). ¹³C NMR (100 MHz, CDCl₃): δ 177.60, 168.98, 155.60, 148.67, 148.07, 146.50, 136.40, 129.41, 128.91, 128.75, 128.56, 127.85, 127.02, 124.10, 122.76, 122.19, 120.91, 119.82, 109.96, 55.54, 55.45, 46.43, 41.80, 38.48, 37.40, 37.10, 36.58, 33.66, 24.05, 23.74, 23.40, 23.00, 18.26, 16.44. HR-MS (*m/z*) (ESI): calcd for C₃₆H₄₃N₃O₄ [M+H⁺]: 582.33318; found: 582.33128.

Compound **9d**: Yields 81.5%; ¹H NMR (400 MHz, CDCl₃) δ 8.30 (s, 1H, NH), 8.21 (s, 1H, NH), 7.65 (s, 1H), 7.29–7.22 (m, 2H), 7.21 (s, 2H), 7.20–7.15 (m, 3H), 7.05–6.90 (m, 2H), 6.81 (d, *J* = 8.1 Hz, 1H), 6.51 (d, *J* = 7.4 Hz, 1H), 4.90–4.84 (m, 1H), 3.69 (s, 3H, OCH₃), 3.18 (d, *J* = 7.0 Hz, 2H), 2.90–2.83 (m, 1H), 2.62–2.51 (m, 2H), 2.28 (d, *J* = 11.0 Hz, 1H), 2.20 (dd, *J* = 11.2, 7.3 Hz, 1H), 1.73–1.50 (m, 5H), 1.33 (s, 3H, CH₃), 1.24 (s, 3H, CH₃), 1.22 (s, 3H, CH₃), 1.10 (s, 3H, CH₃). ¹³C NMR (100 MHz, CDCl₃) δ 177.16, 168.89, 152.95, 148.11, 146.91,

136.44, 132.43, 130.88, 129.30, 128.67, 127.01, 126.92, 125.01, 124.18, 123.23, 120.87, 119.86, 110.00, 55.65, 55.32, 46.40, 43.80, 38.33, 37.29, 37.22, 36.99, 33.59, 23.82, 23.76, 23.74, 23.45, 18.30, 16.35. HR-MS (m/z) (ESI): calcd for $C_{36}H_{43}N_3O_4$ [$M+H^+$]: 582.33318; found: 582.33296.

Compound **9e**: Yields 78%; 1H NMR (400 MHz, $CDCl_3$): δ 8.44 (s, 1H, NH), 7.67 (s, 1H, NH), 7.31–7.27 (m, 1H), 7.25–7.22 (m, 3H), 7.19–7.17 (d, $J = 4.3$ Hz, 3H), 7.16–7.12 (m, 3H), 6.78 (d, $J = 7.6$ Hz, 1H), 6.72–6.68 (m, 2H), 4.96–4.90 (m, 1H), 3.75 (s, 3H, OCH_3), 3.22–3.14 (m, 2H), 2.81–2.63 (m, 3H), 2.37–2.32 (m, 1H), 2.25 (d, $J = 11.5$ Hz, 1H), 1.72–1.55 (m, 5H), 1.34 (s, 3H, CH_3), 1.19 (s, 3H, CH_3), 1.18 (s, 3H, CH_3), 1.11 (s, 3H, CH_3). ^{13}C NMR (100 MHz, $CDCl_3$): δ 177.67, 169.08, 156.53, 152.95, 146.90, 136.45, 132.48, 130.78, 130.33, 129.29, 129.21, 128.86, 128.64, 127.27, 125.03, 123.25, 121.95, 114.01, 55.41, 55.36, 46.38, 43.53, 38.44, 37.20, 37.17, 37.09, 36.92, 33.57, 23.80, 23.72, 18.19, 16.30. HR-MS (m/z) (ESI): calcd for $C_{36}H_{43}N_3O_4$ [$M+H^+$]: 582.33318; found: 582.33051.

Compound **9f**: Yields 81.35%; 1H NMR (400 MHz, $CDCl_3$): δ 8.51 (s, 1H, NH), 7.65 (s, 1H, NH), 7.25 (d, $J = 18.5$ Hz, 1H), 7.21–7.19 (m, 2H), 7.19–7.17 (d, $J = 1.1$ Hz, 3H), 7.17–7.15 (m, 3H), 6.72–6.67 (m, 3H), 4.93–4.88 (m, 1H), 3.72 (s, 3H, OCH_3), 3.23–3.12 (m, 2H), 2.85–2.78 (m, 1H), 2.59 (d, $J = 9.3$ Hz, 2H), 2.27–2.13 (m, 2H), 1.71–1.46 (m, 5H), 1.29 (s, 3H, CH_3), 1.20 (s, 3H, CH_3), 1.19 (s, 3H, CH_3), 1.07 (s, 3H, CH_3). ^{13}C NMR (100 MHz, $CDCl_3$): δ 178.39, 169.23, 156.45, 155.44, 148.55, 146.48, 136.54, 130.45, 129.23, 128.87, 128.67, 127.85, 127.08, 122.77, 122.20, 122.00, 113.94, 55.39, 55.17, 46.49, 42.33, 37.95, 37.41, 37.11, 36.61, 33.66, 24.01, 23.75, 23.34, 22.99, 18.23, 16.32. HR-MS (m/z) (ESI): calcd for $C_{36}H_{43}N_3O_4$ [$M+H^+$]: 582.33318; found: 582.33142.

Compound **9g**: Yields 72.5%; 1H NMR (400 MHz, $CDCl_3$): δ 8.30 (s, 1H, NH), 7.97–7.93 (m, 1H), 7.51 (d, $J = 3.6$ Hz, 1H), 7.12 (s, 2H), 7.03 (d, $J = 8.2$ Hz, 3H), 6.95–6.91 (m, 2H), 6.88–6.81 (m, 2H), 6.49 (d, $J = 7.5$ Hz, 1H), 4.89–4.84 (m, 1H), 3.07–2.99 (m, 2H), 2.70–2.67 (m, 1H), 2.49–2.40 (m, 2H), 2.26–2.20 (m, 1H), 2.01–1.97 (m, 1H), 1.55–1.42 (m, 5H), 1.17 (s, 3H, CH_3), 1.07 (s, 3H, CH_3), 1.05 (s, 3H, CH_3), 0.97 (s, 3H, CH_3). ^{13}C NMR (100 MHz, $CDCl_3$): δ 178.35, 169.79, 155.49, 151.70, 148.67, 146.48, 136.07, 129.42, 129.30, 129.13, 128.82, 128.65, 128.51, 127.84, 127.19, 125.70, 124.88, 124.31, 122.80, 122.40, 122.22, 55.03, 46.44, 42.22, 41.56, 37.83, 37.41, 37.00, 36.60, 36.52, 33.66, 24.08, 23.78, 22.99, 18.20, 16.40. HR-MS (m/z) (ESI): calcd for $C_{35}H_{40}FN_3O_3$ [$M+H^+$]: 570.31320; found: 570.31218.

Compound **9h**: Yields 76.55%; 1H NMR (400 MHz, $CDCl_3$): δ 8.38 (s, 1H, NH), 8.00–7.94 (m, 1H), 7.52–7.50 (m, 1H), 7.11 (d, $J = 6.2$ Hz, 2H), 7.02 (d, $J = 8.1$ Hz, 3H), 6.95–6.89 (m, 2H), 6.87–6.80 (m, 2H), 6.46 (d, $J = 7.4$ Hz, 1H), 4.87–4.81 (m, $J = 14.4, 7.3$ Hz, 1H), 3.09–3.00 (m, 2H), 2.73–2.69 (m, 1H), 2.50–2.40 (m, 2H), 2.13–2.09 (m, 1H), 2.01–1.97 (m, 1H), 1.55–1.32 (m, 5H), 1.16 (s, 3H, CH_3), 1.10 (s, 3H, CH_3), 1.08 (s, 3H, CH_3), 0.94 (s, 3H, CH_3). ^{13}C NMR (100 MHz, $CDCl_3$): δ 178.47, 169.86, 155.30, 151.72, 148.54, 146.46, 136.25, 129.29, 129.11, 128.92, 128.78, 128.70, 127.77, 127.16, 125.67, 124.81, 124.26, 122.73, 122.40, 122.24, 115.04, 114.85, 55.13, 46.46, 42.31, 41.62, 37.84, 37.50, 37.11, 36.62, 33.67, 24.07, 23.78, 23.34, 22.97, 18.25, 16.33. HR-MS (m/z) (ESI): calcd for $C_{35}H_{40}FN_3O_3$ [$M+H^+$]: 570.31320; found: 570.31293.

Compound **9i**: Yields 82.45%; 1H NMR (400 MHz, $CDCl_3$): δ 8.85 (s, 1H, NH), 7.68 (d, $J = 1.6$ Hz, 1H), 7.25–7.20 (m, 4H), 7.19–7.17 (m, 3H), 7.13–7.02 (m, 1H), 6.81–6.76 (m, 3H), 5.00–4.94 (m, 1H), 3.21–3.10 (m, 2H), 2.83–2.58 (m, 3H), 2.34 (dd, $J = 13.2, 5.3$ Hz, 1H), 2.26 (d, $J = 11.6$ Hz, 1H), 1.69–1.52 (m, 5H), 1.34 (s, 3H, CH_3), 1.19 (s, 3H, CH_3), 1.18 (s, 3H, CH_3), 1.12 (s, 3H, CH_3). ^{13}C NMR (100 MHz, $CDCl_3$): δ 178.35, 169.43, 160.59, 158.17, 155.56, 148.66, 146.62, 136.03, 133.35, 129.37, 128.65, 128.03, 127.12, 122.88, 122.19, 122.10, 122.03, 115.44, 115.22, 55.21, 46.46, 41.88, 38.61, 37.47, 37.05, 36.55, 33.65, 23.97, 23.71, 23.50, 22.99, 18.14, 16.39. HR-MS (m/z) (ESI): calcd for $C_{35}H_{40}FN_3O_3$ [$M+H^+$]: 568.29755; found: 568.29608.

Compound **9j**: Yields 84.5%; 1H NMR (400 MHz, $CDCl_3$): δ 8.94 (s, 1H, NH), 7.65 (d, $J = 1.5$ Hz, 1H), 7.23–7.19 (m, 3H), 7.19–7.16 (m, 4H), 7.15 (d, $J = 1.7$ Hz, 1H), 6.79–6.76 (m, 2H), 6.70 (d, $J = 7.6$ Hz, 1H), 4.97–4.89 (m, 1H), 3.25–3.10 (m, 2H), 2.85–2.78 (m, 1H), 2.59 (d, $J = 8.3$ Hz, 2H), 2.26 (d, $J = 11.4$ Hz, 1H), 2.19–2.14 (m, 1H), 1.73–1.45 (m, 5H), 1.30 (s, 3H, CH_3), 1.19 (s, 3H, CH_3), 1.17 (s, 3H, CH_3), 1.07 (s, 3H, CH_3). ^{13}C NMR (100 MHz, $CDCl_3$): δ 178.69, 169.48, 160.53, 158.11, 155.38, 148.49, 146.56, 136.31, 133.40, 129.18, 128.78, 128.67, 127.93, 127.12, 122.79, 122.20, 121.92, 121.84, 115.40, 115.17, 55.21, 46.53, 42.34, 37.91, 37.38, 37.10, 36.59, 33.64, 23.97, 23.73, 23.34, 22.95, 18.20, 16.28. HR-MS (m/z) (ESI): calcd for $C_{35}H_{40}FN_3O_3$ [$M+H^+$]: 570.31320; found: 570.31152.

Compound **9k**: Yields 79.45%; 1H NMR (400 MHz, $CDCl_3$): δ 8.35 (s, 1H, NH), 7.66 (d, $J = 4.6$ Hz, 1H), 7.32–7.29 (m, 2H), 7.25–7.20 (m, 3H), 7.19–7.16 (m, 3H), 7.08–6.99 (m, 2H), 6.41 (d, $J = 7.3$ Hz, 1H), 4.94–4.89 (m, 1H), 3.24–3.16 (m, 2H), 2.90–2.85 (m, 1H), 2.63–2.54 (m, 2H), 2.35–2.27 (m, 1H), 2.14 (d, $J = 8.6$ Hz, 1H), 1.72–1.48 (m, 5H), 1.32 (s, 3H, CH_3), 1.25 (s, 3H, CH_3), 1.23 (s, 3H, CH_3), 1.09 (s, 3H, CH_3). ^{13}C NMR (100 MHz, $CDCl_3$): δ 177.58, 169.34, 152.83, 146.93, 136.13, 134.08, 132.43, 130.85, 129.14, 129.11, 128.85, 127.55, 127.27, 125.09, 124.33, 123.36, 123.19, 121.87, 55.33, 46.47, 43.89, 37.77, 37.31, 37.23, 37.12, 36.96, 33.59, 23.83, 23.77, 23.74, 18.27, 16.34. HR-MS (m/z) (ESI): calcd for $C_{35}H_{40}ClN_3O_3$ [$M+H^+$]: 586.28364; found: 586.28209.

Compound **9l**: Yields 83.45%; 1H NMR (400 MHz, $CDCl_3$): δ 8.36 (s, 1H, NH), 7.66 (d, $J = 1.6$ Hz, 1H), 7.32–7.28 (m, 2H), 7.25–7.21 (m, 3H), 7.19–7.15 (m, 3H), 7.10–6.98 (m, 2H), 6.42 (d, $J = 7.4$ Hz, 1H), 4.95–4.90 (m, 1H), 3.27–3.16 (m, 2H), 2.90–2.84 (m, 1H), 2.65–2.55 (m, 2H), 2.25 (d, $J = 4.7$ Hz, 1H), 2.14 (d, $J = 8.4$ Hz, 1H), 1.68–1.48 (m, 5H), 1.31 (s, 3H, CH_3), 1.25 (s, 3H, CH_3), 1.23 (s, 3H, CH_3), 1.08 (s, 3H, CH_3). ^{13}C NMR (100 MHz, $CDCl_3$): δ 178.28, 169.57, 155.33, 148.51, 146.52, 136.18, 134.20, 129.11, 128.88, 128.83, 127.83, 127.46, 127.28, 125.00, 123.52, 122.74, 122.22, 121.93, 55.24, 46.44, 42.18, 37.63, 37.43, 37.08, 36.59, 33.69, 24.10, 23.81, 23.39, 18.25, 16.44. HR-MS (m/z) (ESI): calcd for $C_{35}H_{40}ClN_3O_3$ [$M+H^+$]: 586.28364; found: 586.28221.

Compound **9m**: Yields 81.45%; 1H NMR (400 MHz, $CDCl_3$): δ 8.64 (s, 1H, NH), 7.54 (d, $J = 1.6$ Hz, 1H), 7.14–7.08 (m, 4H), 7.07–7.01 (m, 4H), 6.93 (d, $J = 8.8$ Hz, 2H), 6.58 (d, $J = 7.4$ Hz, 1H), 4.82–4.77 (m, 1H), 3.04–3.01 (m, 2H), 2.70 (d, $J = 6.9$ Hz, 1H), 2.59–2.46 (m, 2H), 2.24–2.19 (m, 1H), 2.14 (d, $J = 12.5$ Hz, 1H), 1.59–1.42 (m, 5H), 1.21 (s, 3H, CH_3), 1.08 (s, 3H, CH_3), 1.06 (s, 3H, CH_3), 0.99 (s, 3H, CH_3). ^{13}C NMR (100 MHz, $CDCl_3$): δ 178.45, 169.37, 155.56, 148.63, 146.64, 136.01, 135.96, 129.31, 128.75, 128.73, 128.47, 128.12, 127.18, 122.88, 122.16, 121.37, 121.08, 55.30, 46.50, 41.90, 38.35, 37.44, 37.07, 36.55, 33.65, 23.99, 23.73, 23.42, 22.99, 18.16, 16.37. HR-MS (m/z) (ESI): calcd for $C_{35}H_{40}ClN_3O_3$ [$M+H^+$]: 586.28364; found: 586.28126.

Compound **9n**: Yields 82.75%; 1H NMR (400 MHz, $CDCl_3$): δ 9.06 (s, 1H, NH), 7.65 (d, $J = 1.5$ Hz, 1H), 7.22–7.19 (m, 4H), 7.17–7.13 (m, 4H), 7.04–7.01 (m, 2H), 6.69 (d, $J = 7.6$ Hz, 1H), 4.99–4.94 (m, 1H), 3.22–3.08 (m, 2H), 2.84–2.79 (m, 1H), 2.62–2.56 (m, 2H), 2.27 (d, $J = 12.1$ Hz, 1H), 2.19–2.14 (m, 1H), 1.70–1.45 (m, 5H), 1.30 (s, 3H, CH_3), 1.19 (s, 3H, CH_3), 1.18 (s, 3H, CH_3), 1.08 (s, 3H, CH_3). ^{13}C NMR (100 MHz, $CDCl_3$): δ 178.75, 169.63, 155.34, 148.47, 146.59, 136.19, 136.06, 129.15, 128.65, 127.98, 127.14, 122.80, 122.20, 121.24, 55.26, 46.52, 42.33, 38.01, 37.41, 37.09, 36.58, 33.64, 24.01, 23.74, 23.38, 22.96, 18.19, 16.30. HR-MS (m/z) (ESI): calcd for $C_{35}H_{40}ClN_3O_3$ [$M+H^+$]: 586.28364; found: 586.28209.

Compound **9o**: Yields 83.25%; 1H NMR (400 MHz, $CDCl_3$): δ 8.75 (s, 1H, NH), 7.64 (s, 1H, NH), 7.23–7.19 (m, 2H), 7.18–7.14 (m, 5H), 6.58 (d, $J = 4.1$ Hz, 3H), 4.87–4.81 (m, 1H), 3.74 (d, $J = 5.0$ Hz, 9H, $3 \times OCH_3$), 3.12 (d, $J = 7.3$ Hz, 2H), 2.82–2.74 (m, 1H), 2.69–2.50 (m, 2H), 2.34–2.25 (m, 2H), 1.74–1.54 (m, 5H), 1.30 (s, 3H, CH_3), 1.15 (s, 3H, CH_3), 1.13 (s, 3H, CH_3), 1.10 (s, 3H, CH_3). ^{13}C NMR (100 MHz, $CDCl_3$): δ 178.63, 169.46, 155.76, 152.91, 148.61, 146.54, 136.03,

134.41, 133.64, 129.19, 128.86, 128.60, 128.08, 127.15, 122.92, 122.15, 97.51, 60.87, 55.92, 55.39, 46.46, 42.12, 37.96, 37.07, 36.57, 33.62, 23.98, 23.68, 22.99, 18.17, 16.23. HR-MS (m/z) (ESI): calcd for $C_{38}H_{47}ClN_3O_6$ [$M+H^+$]: 642.35431; found: 642.35226.

Compound **9p**: Yields 80.55%; 1H NMR (400 MHz, $CDCl_3$): δ 8.87 (s, 1H, NH), 7.64 (s, 1H, NH), 7.22–7.19 (m, 3H), 7.18–7.12 (m, 4H), 6.65 (s, 2H), 6.56 (d, $J = 6.9$ Hz, 1H), 4.85–4.80 (m, 1H), 3.75 (s, 3H, OCH_3), 3.69 (s, 6H, $2 \times OCH_3$), 3.20–3.10 (m, 2H), 2.84–2.77 (m, 1H), 2.60 (d, $J = 9.4$ Hz, 2H), 2.24 (d, $J = 12.5$ Hz, 1H), 2.09 (d, $J = 8.6$ Hz, 1H), 1.69–1.40 (m, 5H), 1.27 (s, 3H, CH_3), 1.19 (s, 3H, CH_3), 1.18 (s, 3H, CH_3), 1.05 (s, 3H, CH_3). ^{13}C NMR (100 MHz, $CDCl_3$): δ 178.94, 169.57, 155.36, 152.99, 148.50, 146.58, 136.40, 134.45, 133.72, 129.02, 128.81, 127.93, 127.16, 122.84, 122.13, 97.50, 60.89, 55.93, 55.63, 46.47, 42.42, 37.48, 37.32, 37.05, 36.61, 33.65, 24.03, 23.75, 23.39, 22.95, 18.19, 16.30. HR-MS (m/z) (ESI): calcd for $C_{38}H_{47}ClN_3O_6$ [$M+H^+$]: 642.35431; found: 642.35346.

4.4. Cell lines and culture

The NCI–H460 (human lung cancer cell), HeLa (epithelial cervical) and MGC-803 (gastric) human cancer cell lines used in this study were all obtained from the Institute of Biochemistry and Cell Biology, China Academy of Sciences. They were maintained in DMEM medium; all were supplemented with 10% heat-inactivated fetal bovine serum in a humidified atmosphere of 5% CO_2 at 37 °C.

4.5. MTT assay against cancer cell viability

MTT assay was performed as described previously [47]. All tested compounds were dissolved in DMSO and subsequently diluted in culture medium before treatment of cultured cells. Tested cells were plated in 96-well plates at a density of 5×10^3 cells/well per 180 μ L of the proper culture medium and treated with the compounds at 20 μ M for 48 h. In parallel, the cells treated with 0.1% DMSO served as negative control and those treated with 5-FU as positive control. Finally, 10 μ L of MTT was added, and the cells were incubated for 4 h. After removal of the supernatant, DMSO (100 mL) was added to dissolve the formazan crystals. The absorbance was read by enzyme labeling instrument with 570/630 nm double wavelength measurement. The cytotoxicity was estimated based on the percentage cell survival in a dose dependent manner relative to the negative control. The final IC_{50} values were calculated by the Bliss method ($n = 5$). All the tests were repeated in at least three independent experiments.

4.6. AO/EB staining

The procedure was performed as described previously [47]. Cells were seeded at a concentration of 5×10^4 cell/mL in a volume of 2 mL on a sterile cover slip in six-well tissue culture plates. Following incubation, the medium was removed and replaced with fresh medium plus 10% fetal bovine serum and supplemented with compound **8K** (15 μ M). After the treatment period, the cover slip with monolayer cells was inverted on a glass slide with 20 μ L of AO/EB stain (100 mg/mL). Fluorescence was read on a Nikon ECLIPSETE2000-S fluorescence microscope (OLYMPUS Co., Japan).

4.7. Hoechst 33258 staining

Hoechst 33258 staining assay was performed as described previously [47]. Cells grown on a sterile cover slip in six-well tissue culture plates were treated with compounds for a certain range of time. The culture medium containing compounds was removed, and the cells were fixed in 4% paraformaldehyde for 10 min. After being washed twice with PBS, the cells were stained with 0.5 mL of

Hoechst 33258 (Beyotime) for 5 min and then again washed twice with PBS. The stained nuclei were observed under an Nikon ECLIPSETE2000-S fluorescence microscope using 350 nm excitation and 460 nm emission.

4.8. Mitochondrial membrane potential staining

The assay was performed as described previously [47]. JC-1 probe was employed to measure mitochondrial depolarization in HeLa cells. Briefly, Cells cultured in six-well plates after indicated treatments were incubated with an equal volume of JC-1 staining solution (5 μ g/mL) at 37 °C for 20 min and rinsed twice with PBS. Mitochondrial membrane potentials were monitored by determining the relative amounts of dual emissions from mitochondrial JC-1 monomers or aggregates using an Nikon ECLIPSETE2000-S fluorescent microscope. Mitochondrial depolarization is indicated by an increase in the green/red fluorescence intensity ratio.

4.9. TUNEL assay

TUNEL assay was performed as described previously [47]. The TUNEL method was performed to label 3'-end of fragmented DNA of the apoptotic HeLa cells. The cells treated as indicated were fixed with 4% paraform phosphate buffer saline, rinsed with PBS, then permeabilized by 0.1% Triton X-100 for FITC end-labeling the fragmented DNA of the apoptotic HeLa cells using TUNEL cell apoptosis detection kit. The FITC-labeled TUNEL-positive cells were imaged under a fluorescent microscopy by using 488 nm excitation and 530 nm emission.

4.10. Apoptosis assays by flow cytometry assay

Prepared HeLa cells (1×10^6 cells/mL) were washed twice with cold PBS and then resuspended gently in 500 μ L of binding buffer. Thereafter, cells were stained in 5 μ L of Annexin V-FITC and shaken well. Finally, the cells were mixed with 5 μ L of PI, incubated for 20 min in the dark and subsequently analyzed using FACSCalibur (Becton Dickinson).

4.11. Cell cycle analysis

Cell cycle analysis was performed as described previously [47]. HeLa cell lines were maintained in Dulbecco's modified Eagle's medium with 10% fetal calf serum in 5% CO_2 at 37 °C. Cells were harvested by trypsinization and rinsed with PBS. After centrifugation, the pellet (10^5 – 10^6 cells) was suspended in 1 mL of PBS and kept on ice for 5 min. The cell suspension was then fixed by the dropwise addition of 9 mL precooled (4 °C) 70% ethanol with violent shaking. Fixed samples were kept at 4 °C until use. For staining, cells were centrifuged, resuspended in PBS, digested with 150 mL of RNase A (250 mg/mL), and treated with 150 mL of pro-pidium iodide (PI) (0.15 mM), then incubated for 30 min at 4 °C. PI-positive cells were counted with a FACScan Fluorescence-activated cell sorter (FACS). The population of cells in each cell cycle phase was determined using Cell Modifit software (Becton Dickinson).

4.12. Cytochrome c release assay

Cytochrome c release assay was performed as described previously [47]. Cells were cultured in six-well plates with different concentrations of the drug. The culture medium containing compounds was removed, and the cells were fixed in 4% paraformaldehyde for 1 h. Using immunol staining wash buffer washed 3 times, 5 min each. Slow shaking at room temperature with blocking solution for 3 h. Exhaustion blocking solution and

immediately joined diluted primary antibody (1:500) incubated for 1 h. Immunol staining wash buffer washed for 3 times, 5 min each. Exhaustion washing liquid and added into diluted secondary antibody (1:500) incubated for 1 h at room temperature. Punctate or granular nature of fluorescence was observed at Nikon ECLIP-SETE2000-S fluorescence microscope using 550 nm excitation and 570 nm emission.

4.13. ROS generation assay

ROS generation assay was performed as described previously [47]. Intracellular ROS generation was investigated using dichlorodihydro fluorescein diacetate (DCFH-DA) assay. DCFH-DA is taken up by cells, and then activated by esterase-mediated cleavage of acetate to form dichlorodihydro fluorescein (DCFH), which is trapped in the cells. DCFH is converted to fluorescein DCF in the presence of ROS. HeLa cells were seeded in six-well plates with about 60% confluence. Following incubation with 10 μ M 4b for 24 h, cells were treated with 10 μ M DCFH-DA. After 15 min incubation, cells were washed twice with PBS and then exposed to light. Immediately after light exposure, cell images were acquired using an inverted fluorescence microscope.

4.14. Caspase-3 and -9 activities assay

The assay was performed as described previously [47]. Caspases activities were determined using Caspase Activity Kit (Beyotime, China) according to the manufacturer's instructions. Briefly, cells were collected, washed with cold PBS and suspended in lysis buffer for 15 min on ice. Lysates were centrifuged at 16,000 g for 15 min at 4 °C. The protein concentration of the extracts was determined using the Bradford method. Activities of caspase-3 and -9 were measured by cleavage of substrate peptides Ac-DEVD-pNA and Ac-LEHD-pNA to yellow formazan product, p-nitroaniline (pNA), which was quantified on a scanning multi-well spectrophotometer at an absorbance of 405 nm.

4.15. Determination of caspase-3 activity

The test was performed as described previously [47]. The activation of caspase-3 was examined using a caspase-3 (DEVD-FMK) conjugated to FITC as the fluorescent in situ marker in living cells (catalog #QIA91, Merck). FITC-DEVD-FMK is cell permeable, nontoxic, and irreversibly binds to activated caspase-3 in apoptotic cells. After exposure of HeLa cell lines to compound 8k for 8 h, the cultures were washed twice with HBSS containing 0.1% BSA and then incubated with FITC-DEVD-FMK (1 mL/mL in EBSS) for 1 h in a 37 °C incubator with 5% CO₂. The FITC label in apoptotic cells was examined immediately under fluorescent microscope with excitation and emission at 485 and 535 nm, respectively (25 × , Nikon).

4.16. Western blot assay

Western blot analysis was performed as described previously [48]. After the treatments, the cells were washed in PBS and then lysed with RIPA (radioimmunoprecipitation assay) buffer (Tris–Cl [50 mM], NaCl [150 mM], sodium dodecyl sulfate [SDS; 0.1%]) containing proteinase inhibitor cocktail and phosphatase inhibitor cocktail (Roche, Indianapolis, IN). The lysate was centrifuged at 3000 g at 4 °C for 10 min. The supernatants were collected, and the protein concentrations were determined using a BCA Protein Assay kit (Pierce, Rockford, IL). A 50 μ g sample of proteins was separated by 12% SDS–polyacrylamide gel electrophoresis (SDS–PAGE), and the resolved proteins were transferred to a methylcellulose membrane (Millipore, Billerica, MA). The membrane was blocked with

5% nonfat milk in Tris-buffered saline containing 0.1% Tween-20 (TBST) at room temperature for 1 h and then incubated with the primary antibodies at 4 °C overnight. After being washed with TBST, the membrane was incubated with anti-mouse or anti-rabbit horseradish peroxidase-conjugated secondary antibodies. Antibodies against caspases 3 (dilution 1:1000) or tubulin (dilution 1:10,000) were incubated overnight at 4 °C. The secondary antibodies (dilution 1:5000) were incubated for 2 h at room temperature. After washing, the membranes were exposed to enhanced chemoluminescent (ECL) reagent. BioMax film was used for Western blotting. The blots were quantified by laser scanning densitometry.

4.17. Statistical analysis

All statistical analysis was performed with SPSS Version 10. Data was analyzed by one-way ANOVA. Mean separations were performed using the least significant difference method. Each experiment was replicated thrice, and all experiments yielded similar results. Measurements from all the replicates were combined, and treatment effects were analyzed.

Acknowledgments

This study was supported by the National Natural Science Foundation of China (No. 81260472 21362002 and 21431001), Guangxi Natural Science Foundation of China (No. 2014GXNSFDA118007 and 2014GXNSFBA118050), "BAGUI Scholar" Project, the State Key Laboratory Cultivation Base for the Chemistry and Molecular Engineering of Medicinal Resources, Ministry of Science and Technology of China (CMEMR2014-B and CMEMR2014-A02), the Fundamental Research Funds for the Central Universities and the Foundation of Ministry of Education Innovation Team (NO. IRT1225).

Appendix A. Supplementary data

Supplementary data related to this article can be found at <http://dx.doi.org/10.1016/j.ejmech.2014.10.060>.

References

- [1] K.H. Son, H.M. Oh, S.K. Choi, D.C. Han, B.M. Kwon, *Bioorg. Med. Chem. Lett.* 15 (2005) 2019–2021.
- [2] D.J. Newman, G.M. Cragg, K.M. Snader, *J. Nat. Prod.* 66 (2003) 1022–1037.
- [3] E.L. Cooper, J. Evid. Based Complement. Altern. Med. 1 (2004) 215–217.
- [4] C.F. Chyu, H.C. Lin, Y.H. Kuo, *Chem. Pharm. Bull.* 53 (2005) 11–14.
- [5] H. Wada, S. Kodato, M. Kawamori, T. Morikawa, H. Nakai, M. Takeda, S. Saito, Y. Onoda, H. Tamaki, *Chem. Pharm. Bull.* 33 (1985) 1472–1487.
- [6] (a) S. Savluchinske Feio, J. Carlos Roseiro, B. Gigante, M.J. Marcelo-Curto, *J. Microbiol. Methods* 28 (1997) 201–206; (b) B. Gigante, A.M. Silva, M.J. Marcelo-Curto, S. Savluchinske Feio, J. Roseiro, L.V. Reis, *Planta Med.* 68 (2002) 680–684.
- [7] I.A. Tolmacheva, A.V. Tarantin, A.A. Boteva, L.V. Anikina, Y.B. Vikharev, V.V. Grishko, A.G. Tolstikov, *Pharm. Chem. J.* 40 (2006) 489–493.
- [8] J.R. Tagat, D.V. Nazareno, M.S. Puar, S.W. McCombie, A.K. Ganguly, *Bioorg. Med. Chem. Lett.* 4 (1994) 1101–1104.
- [9] (a) Y. Kinouchi, H. Ohtsu, H. Tokuda, H. Nishino, S. Matsunaga, R. Tanaka, *J. Nat. Prod.* 63 (2000) 817–820; (b) R. Tanaka, H. Tokuda, Y. Ezaki, *Phytomedicine* 15 (2008) 985–992.
- [10] S. Prinz, U. Müllner, J. Heilmann, K. Winkelmann, O. Sticher, E. Haslinger, A. Hüfner, *J. Nat. Prod.* 65 (2002) 1530–1534.
- [11] B. Goodson, A. Ehrhardt, N.G. Simon, J. Nuss, K. Johnson, M. Giedlin, R. Yamamoto, W.H. Moos, A. Krebber, *Antimicrob. Agents Chemother.* 43 (1999) 1429–1434.
- [12] C. H. Lin, H. S. Chuang, US Patent 5, 248, 696 (2003).
- [13] M.A. González, D.P. Guaita, J.C. Royero, B. Zapata, L. Agudelo, A.M. Arango, L.B. Galvis, *Eur. J. Med. Chem.* 45 (2010) 811–816.
- [14] X. Rao, Z. Song, L. He, W. Jia, *Chem. Pharm. Bull.* 56 (2008) 1575–1578.
- [15] (a) X.C. Huang, M. Wang, Y.M. Pan, X.Y. Tian, H.S. Wang, Y. Zhang, *Bioorg. Med. Chem. Lett.* 23 (2013) 5283–5289;

- (b) X.C. Huang, M. Wang, Y.M. Pan, G.Y. Yao, H.S. Wang, X.Y. Tian, J.K. Qin, Y. Zhang, *Eur. J. Med. Chem.* 69 (2013) 508–520.
- [16] (a) F.F. Tian, P. Zhou, Z.L. Li, *J. Mol. Struct.* 830 (2007) 106–115;
(b) T. Day, S.A. Greenfield, *Exp. Brain Res.* 155 (2004) 500–508.
- [17] B. Leader, Q.J. Baca, D.E. Golan, *Nat. Rev. Drug Discov.* 7 (2008) 21–39.
- [18] R.E.W. Hancock, M.G. Scott, *Proc. Natl. Acad. Sci. U S A* 97 (2000) 8856–8861.
- [19] A.I. Faden, V.A. Movsesyan, S.M. Knoblach, F. Ahmed, I. Cernak, *Neuropharmacology* 49 (2005) 410–424.
- [20] P.E. Nielsen, *Pseudo-peptides in Drug Discovery*, Wiley, New York, 2004.
- [21] J.Z. Liu, B.A. Song, H.T. Fan, P.S. Bhadury, W.T. Wan, S. Yang, W.M. Xu, J. Wu, L.H. Jin, X. Wei, D.Y. Hu, S. Zeng, *Eur. J. Med. Chem.* 45 (2010) 5108–5112.
- [22] M. Masquelier, R. Baurain, A. Trouet, *J. Med. Chem.* 23 (1980) 1166–1170.
- [23] C. Ryppa, H. Steinberg, M. Biniossek, R. Fainaro, F. Kratz, *Int. J. Pharm.* 368 (2009) 89–97.
- [24] S. Zitzmann, V. Ehemann, M. Schwab, *Cancer Res.* 62 (2002) 5139–5143.
- [25] Y. Hensbergen, H.J. Broxterman, Y.W. Elderkamp, J. Lankelma, J.C. Beers, M. Heijn, E. Boven, K. Hoekman, H.M. Pinedo, *Biochem. Pharmacol.* 63 (2002) 897–908.
- [26] K. Breistol, H.R. Hendriks, D.P. Berger, S.P. Langdon, H.H. Fiebig, O. Fodstad, *Eur. J. Cancer* 34 (1998) 1602–1606.
- [27] Soo-Jeong Choi, Jung-Eun Lee, Soon-Young Jeong, Isak Im, So-Deok Lee, Eun-Jin Lee, Sang Kook Lee, Seong-Min Kwon, Sang-Gun Ahn, Jung-Hoon Yoon, Sun-Young Han, Jae-Il Kim, Yong-Chul Kim, *J. Med. Chem.* 53 (2010) 3696–3706.
- [28] Rubing Wang, Xu Zhang, Hualong Song, Shanshan Zhou, Shaoshun Li, *Bioorg. Med. Chem. Lett.* 24 (2014) 4304–4307.
- [29] X.C. Huang, M. Wang, H.S. Wang, Z.F. Chen, Y. Zhang, Y.M. Pan, *Bioorg. Med. Chem. Lett.* 24 (2014) 1511–1518.
- [30] M. Al. H. Hassan, A.E. Fahamb, G. Mohamed, A.F. Khalid, *Arab. J. Chem.* 5 (2012) 285–289.
- [31] Y.-M. Cui, E. Yasutomi, Y. Otani, T. Yoshinaga, K. Ido, K. Sawada, T. Ohwada, *Bioorg. Med. Chem. Lett.* 18 (2008) 5201–5205.
- [32] F. Bunz, *Curr. Opin. Pharmacol.* 1 (2001) 337–341.
- [33] (a) S.H. Kaufmann, W.C. Earnshaw, *Exp. Cell. Res.* 256 (2000) 42–49;
(b) S. Fulda, K.M. Debatin, *Oncogene* 25 (2006) 4798–4811.
- [34] A. Thorburn, *Cell. Signal.* 16 (2004) 139–144.
- [35] E. Emine, L. Oliver, P.F. Cartron, P. Juin, S. Manon, F.M. Vallette, *Biochim. Biophys. Acta-Bioenergetics* 1757 (2006) 1301–1311.
- [36] J.S. Bose, V. Gangan, R. Prakash, S.K. Jain, S.K. Manna, *J. Med. Chem.* 52 (2009) 3184–3190.
- [37] J.Y. Zhang, H.Y. Wu, X.K. Xia, Y.J. Liang, Y.Y. Yan, Z.G. She, Y.C. Lin, L.W. Fu, *Cancer Biol. Ther.* 6 (2007) 1413–1421.
- [38] Z. Quan, J. Gu, P. Dong, J. Lu, X. Wu, W. Wu, X. Fei, S. Li, Y. Wang, J. Wang, Y. Liu, *Cancer Lett.* 295 (2010) 252–259.
- [39] X.H. Wang, D.Z. Jia, Y.J. Liang, S.L. Yan, Y. Ding, L.M. Chen, Z. Shi, M.S. Zeng, G.F. Liu, L.W. Fu, *Cancer Lett.* 249 (2007) 256–270.
- [40] N. Zamzami, P. Marchetti, M. Castedo, D. Decaudin, A. Macho, T. Hirsch, S.A. Susin, P.X. Petit, B. Mignotte, G. Kroemer, *J. Exp. Med.* 182 (1995) 367–377.
- [41] D.Z. Liu, Z. Tian, Z.H. Yan, L.X. Wu, Y. Ma, Q. Wang, W. Liu, H.G. Zhou, C. Yang, *Bioorg. Med. Chem.* 21 (2013) 2960–2967.
- [42] C.J. Vickers, G.E. Gonzalez-Paez, D.W. Wolan, *J. Am. Chem. Soc.* 135 (2013) 12869–12876.
- [43] S. Snigdha, E.D. Smith, G.A. Prieto, C.W. Cotman, *Neurosci. Bull.* 28 (2012) 14–24.
- [44] Z.X. Fang, P.C. Liao, Y.L. Yang, F.L. Yang, Y.L. Chen, Y.L. Lam, K.F. Hua, S.H. Wu, *J. Med. Chem.* 53 (2010) 7967–7978.
- [45] H.L. Yang, S.C. Chen, C.S. Chen, S.Y. Wang, Y.C. Hseu, *Food. Chem. Toxicol.* 46 (2008) 3318–3324.
- [46] S.S. Zhang, S.P. Nie, D.F. Huang, Y.L. Feng, M.Y. Xie, *J. Agric. Food Chem.* 62 (2014) 1581–1589.
- [47] M.Y. Ye, G.Y. Yao, Y.M. Pan, Z.X. Liao, Y. Zhang, H.S. Wang, *Synthesis and antitumor activities of novel a-aminophosphonate derivatives containing an alizarin moiety*, *Eur. J. Med. Chem.* 83 (2014) 116–128.
- [48] J.A. Jara, V.C. Castillo, J.S. Olavarria, L. Peredo, M. Pavanni, F. Jan'a, M.E. Letelier, E. Parra, M.L. Becker, A. Morello, U. Kemmerling, J.D. Maya, J. Ferreira, *J. Med. Chem.* 57 (2014) 2440–2454.